TECHNICAL REPORT BRL-TR-3364

BRL

A COMBINED LUMPED PARAMETER/ONE-DIMENSIONAL BLOWDOWN MODEL FOR THE REGENERATIVE LIQUID PROPELLANT GUN

TERENCE P. COFFEE

JUNE 1992

U.S. ARMY LABORATORY COMMAND

BALLISTIC RESEARCH LABORATORY
ABERDEEN PROVING GROUND, MARYLAND

NOTICES

Destroy this report when it is no longer needed. DO NOT return it to the originator.

Additional copies of this report may be obtained from the National Technical Information Service, U.S. Department of Commerce, 5285 Port Royal Road, Springfield, VA 22161.

The findings of this report are not to be construed as an official Department of the Army position, unless so designated by other authorized documents.

The use of trade names or manufacturers' names in this report does not constitute indorsement of any commercial product.

REPORT DOCUMENTATION PAGE

Form Approved
OMB No. 0704-0188

1. AGENCY USE ONLY (Leave blank)	2. REPORT DATE	3. REPORT TYPE AND DATES COVERED
	June 1992	Final, January 1991–June 1991

4. TITLE AND SUBTITLE

A Combined Lumped Parameter/One-Dimensional Blowdown Model for the Regenerative Liquid Propellant Gun

5. FUNDING NUMBERS

PR: 1L162618AH80
DA30 6709

6. AUTHOR(S)

Terence P. Coffee

7. PERFORMING ORGANIZATION NAME(S) AND ADDRESS(ES)

8. PERFORMING ORGANIZATION REPORT NUMBER

9. SPONSORING/MONITORING AGENCY NAME(S) AND ADDRESS(ES)

U.S. Army Ballistic Research Laboratory
ATTN: SLCBR-DD-T
Aberdeen Proving Ground, MD 21005-5066

10. SPONSORING/MONITORING AGENCY REPORT NUMBER

BRL-TR-3364

11. SUPPLEMENTARY NOTES

12a. DISTRIBUTION/AVAILABILITY STATEMENT

Approved for public release; distribution is unlimited.

12b. DISTRIBUTION CODE

13. ABSTRACT *(Maximum 200 words)*

A new model for the regenerative liquid propellant gun has been developed. The model is lumped parameter except for the gun tube, which is one-dimensional. The purpose of the new model is to cover the blowdown phase, after the projectile has exited from the gun tube. The gun tube profiles are then used as input for a thermal management code, which computes the heat transfer to the gun tube.

14. SUBJECT TERMS

liquid gun propellants; concept VIC; regenerative gun; lumped parameter model; blowdown; one-dimensional model

15. NUMBER OF PAGES

32

16. PRICE CODE

17. SECURITY CLASSIFICATION OF REPORT	18. SECURITY CLASSIFICATION OF THIS PAGE	19. SECURITY CLASSIFICATION OF ABSTRACT	20. LIMITATION OF ABSTRACT
UNCLASSIFIED	UNCLASSIFIED	UNCLASSIFIED	UL

INTENTIONALLY LEFT BLANK.

TABLE OF CONTENTS

		Page
	LIST OF FIGURES	v
1.	INTRODUCTION	1
2.	LIQUID GUN CODES	1
3.	NUMERICAL PROCEDURE	2
3.1	Governing Equations	4
3.2	Grid	6
3.3	Heat Loss	8
3.4	Boundary Conditions	10
3.5	Time Step	13
4.	VALIDATION	16
4.1	Comparison With Lumped Parameter Model	16
4.2	Comparison With Theory	21
5.	TEST CASE	23
6.	CONCLUSIONS	34
7.	REFERENCES	35
	DISTRIBUTION LIST	37

INTENTIONALLY LEFT BLANK.

LIST OF FIGURES

Figure		Page
1.	The Grid for the 1-D Gun Tube Model	3
2.	Round 77. Chamber Pressure. Lumped Parameter Model (Line). Coarse Grid (Dot). Finer Grid (Dash)	18
3.	Round 77. Projectile Velocity. Lumped Parameter Model (Line). Coarse Grid (Dot). Finer Grid (Dash)	18
4.	Round 77. Gun Tube Gas Velocity, Time = 18 ms. Lumped Parameter Model (Line). Coarse Grid (Dot). Finer Grid (Dash)	19
5.	Round 77. Gun Tube Gas Pressure, Time = 18 ms. Lumped Parameter Model (Line). Coarse Grid (Dot). Finer Grid (Dash)	19
6.	Round 77. Gun Tube Gas Density, Time = 18 ms. Lumped Parameter Model (Line). Coarse Grid (Dot). Finer Grid (Dash)	20
7.	Round 77. Gun Tube Gas Temperature, Time = 18 ms. Lumped Parameter Model (Line). Coarse Grid (Dot). Finer Grid (Dash)	20
8.	Simple Blowdown. Gun Tube Gas Velocity, Time = 2 ms. Coarse Grid (Line). Medium Grid (Dot). Fine Grid (Dash)	22
9.	Simple Blowdown. Gun Tube Gas Pressure, Time = 2 ms. Coarse Grid (Line). Medium Grid (Dot). Fine Grid (Dash)	22
10.	Simple Blowdown. Gun Tube Gas Velocity, Time = 1.06 ms. One-Dimensional Model (Line). Corner Theory (Dot)	24
11.	Simple Blowdown. Gun Tube Gas Pressure, Time = 1.06 ms. One-Dimensional Model (Line). Corner Theory (Dot)	24
12.	Simple Blowdown. Gun Tube Gas Velocity, Time = 1.5 ms. One-Dimensional Model (Line). Corner Theory (Dot)	25
13.	Simple Blowdown. Gun Tube Gas Pressure, Time = 1.5 ms. One-Dimensional Model (Line). Corner Theory (Dot)	25
14.	Simple Blowdown. Gun Tube Gas Velocity, Time = 2.0 ms. One-Dimensional Model (Line). Corner Theory (Dot)	26
15.	Simple Blowdown. Gun Tube Gas Pressure, Time = 2.0 ms. One-Dimensional Model (Line). Corner Theory (Dot)	26

Figure | Page

16. Test Case. Gun Tube Gas Velocity, Time = 25 ms. Coarse Grid (Line). Medium Grid (Dot). Fine Grid (Dash) 27

17. Test Case. Gun Tube Gas Pressure, Time = 25 ms. Coarse Grid (Line). Medium Grid (Dot). Fine Grid (Dash) 28

18. Test Case. Gun Tube Gas Density, Time = 25 ms. Coarse Grid (Line). Medium Grid (Dot). Fine Grid (Dash) 28

19. Test Case. Gun Tube Gas Temperature, Time = 25 ms. Coarse Grid (Line). Medium Grid (Dot). Fine Grid (Dash) 29

20. Test Case Pressure at Left of Tube (Line). Pressure at Right of Tube (Dot) . 30

21. Test Case. Average Gun Tube Gas Temperature 30

22. Test Case. Gas Velocity at Right of the Tube (Line). Average Speed of Sound in Tube (Dot) 31

23. Test Case. Gun Tube Gas Velocity. Time = 20 ms (Line), 25 ms (Dot), 30 ms (Dash), 35 ms (Dot-Dash) 32

24. Test Case. Gun Tube Gas Velocity. Time = 40 ms (Line), 50 ms (Dot), 60 ms (Dash), 70 ms (Dot-Dash) 32

25. Test Case. Gun Tube Gas Pressure. Time = 20 ms (Line), 25 ms (Dot), 30 ms (Dash), 35 ms (Dot-Dash) 33

26. Test Case. Gun Tube Gas Pressure. Time = 40 ms (Line), 50 ms (Dot), 60 ms (Dash), 70 ms (Dot-Dash) 33

1. INTRODUCTION

Requirements for advanced gun systems, such as the U.S. Army Advanced Field Artillery System (AFAS), include increased firing rates in both burst and sustained firing modes. A serious problem attendant to such capabilities is that of thermal management, which is required to minimize thermal damage and wear tc the tube and associated gun parts, to reduce the effects of thermal distortions on gun tube accuracy, and to eliminate safety problems such as charge or projectile cookoff. A comprehensive approach to the problem involves a careful analysis of the influence of firing rate on both the weapon heating problem and mission effectiveness of each of the propulsion options under consideration. In the case of AFAS, this choice now includes solid and liquid propellants.

A two-dimensional (2-D) gun tube heat conduction code was developed especially to address the current thermal management concerns (Chandra and Fisher 1989a, 1989b; Chandra 1990; Conroy 1990; Keller et al. 1991). This code uses the gas temperature, pressure, and velocity output of an interior ballistics (IB) code as its input. It is assumed that the heat transfer process can be uncoupled from the combustion and flow occurring within the gun tube. The interior ballistics code provides a file containing gas temperature, gas pressure, and gas velocity as a function of time and distance along the gun tube. The IB calculation is continued until the gas temperature and pressure decline to near ambient (i.e., the blowdown phase must be included).

For a solid propellant charge, the XNOVAKTC code (Gough 1980, 1990) is used to generate the required profiles. This report discusses the code developed to run the liquid propellant simulations.

2. LIQUID GUN CODES

Most of the regenerative liquid propellant gun modeling at the U.S. Army Ballistic Research Laboratory (BRL), Aberdeen Proving Ground, MD, has used a lumped parameter code developed in-house (Coffee 1985, 1988; Morrison and Coffee 1990). This code has been extensively validated against experimental data (Coffee, Wren, and Morrison 1989,

1990; Wren, Coffee, and Morrison 1990; Coffee et al. 1991). Some special purpose codes have also been developed—a one-dimensional (1-D) model for the liquid reservoir (Coffee 1988) and a 2-D model for the combustion chamber/gun tube (Coffee, to be published). Also, Gough has written several liquid propellant models—a model that is 1-D in the gun tube and lumped parameter elsewhere (Gough 1987), and a complete 1-D model (Wren and Gough 1991). However, the solution terminates at projectile exit.

The new factor required is the modeling of the blowdown phase. After the projectile exits the gun tube, a rarefaction wave will propagate from the muzzle toward the breech. It is possible to model a rarefaction wave using a lumped parameter code. In fact, the lumped parameter code assumes that a rarefaction wave propagates from the chamber toward the muzzle after burn out of the propellant (Morrison and Coffee 1990). However, rather than modeling two rarefaction waves with a lumped parameter code, a 1-D model in the gun tube was developed. For the rest of the system, the lumped parameter representation is sufficiently accurate.

3. NUMERICAL PROCEDURE

In the Concept VIC regenerative liquid gun, the propellant is initially behind two pistons. The inner or control piston moves first, opening up an annular vent. The outer, or injection, piston then slightly trails the inner piston. The motion of the control piston is modulated by a damper region. Propellant is injected between the pistons into the combustion chamber. The combustion takes place in the combustion chamber, and the gas then flows into the gun tube. Unlike solid propellant guns, there is a large area change from the chamber to the tube.

The governing equations from the lumped parameter model are used for the damper, liquid reservoir, combustion chamber, and projectile. Previous work indicates that very little liquid gets into the gun tube, so for simplicity, the fluid in the tube is assumed to be pure gas.

A staggered grid is used in the gun tube (Figure 1). The velocities are defined at the solid lines. This vector grid is evenly spaced between the gun tube entrance and the projectile. The scalar quantities (pressure, temperature, and density) are defined midway between the

velocities (dotted lines). The grid divides the tube into scalar control volumes (between the solid lines). The scalar quantities are assumed to be uniform in the scalar control volumes, with a discontinuity at the solid lines. Similarly, there are vector control volumes (between the dotted lines). The velocity is assumed to be uniform within vector control volumes. Additional control volumes are established outside the physical gun tube to help set the boundary conditions (see below). The projectile motion is computed in the usual fashion, based on the pressure at the base of the projectile. As the projectile moves, the grid stretches (conformal grid). Additional points are added to the grid as needed.

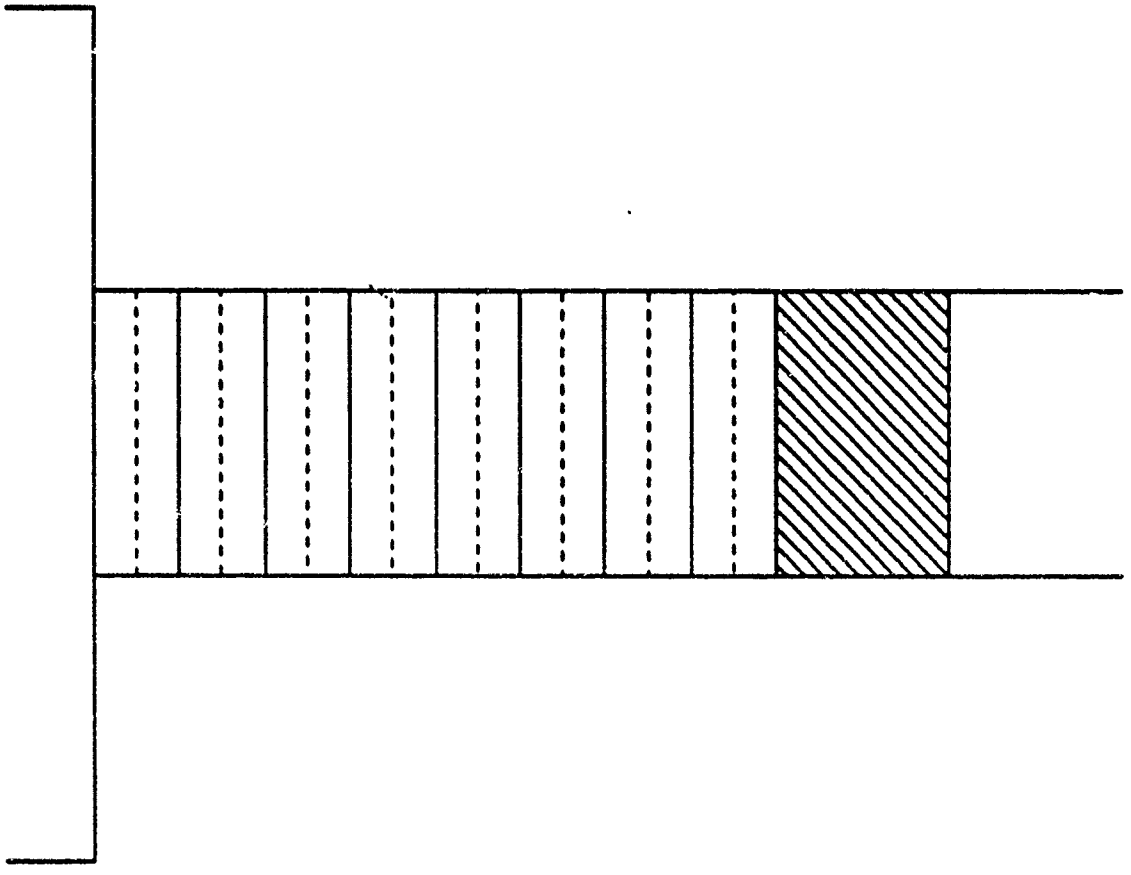

Figure 1. The Grid for the 1-D Gun Tube Model.

The governing equations are cast in integral form. The procedure is inherently conservative. That is, if mass, momentum, or energy leaves one control volume through a boundary, it automatically enters the neighboring control volume. For simplicity, an explicit numerical integration scheme is used. Upwind differencing is used for stability.

3.1 Governing Equations. The 1-D continuity equation is (Bird, Stewart, and Lightfoot 1960)

$$\partial\rho/\partial t + \partial(\rho\, v)/\partial x = 0\,, \tag{1}$$

where ρ is the gas density (g/cm^3) and v is the gas velocity (cm/s). Now consider some volume in three-dimensional (3-D) space. By the divergence theorem, Equation 1 can be written as

$$\begin{aligned} \partial/\partial t \int_V \rho\, dV &= -\int_V (\partial(\rho\, v)/\partial x)\, dV \\ &= -\int_s (\rho\, v\, \boldsymbol{l})\, \boldsymbol{n}\, dS\,. \end{aligned} \tag{2}$$

The first two integrals are volume integrals. The last integral is a surface integral. The vector $\boldsymbol{l}$ is the unit vector in the x (down bore) direction, and $\boldsymbol{n}$ is the unit outward normal vector to the surface. So any change in the mass in the control volume is due to mass flux across a boundary.

The energy equation can be written as (Bird, Stewart, and Lightfoot 1960)

$$\rho\, c_v\, \partial T/\partial t = -\rho\, c_v\, v\, \partial T/\partial x - T\,(\partial p/\partial T)_\rho\ \ (\partial v/\partial x)\,, \tag{3}$$

where T is the temperature (K), c_v is the specific heat at constant volume (J/g – K), and p is the pressure (MPa). The viscous heating term, which is almost always small, is eliminated. The thermal conductivity term is also not included. In the gun tube, the temperature is fairly

constant, and the thermal conductivity term is much smaller than the convection terms. Using the Noble-Abel equation, the derivative of p with respect to T with the density constant is simply the pressure over the temperature. Making this substitution and dividing by the specific heat produces

$$\rho\, \partial T/\partial t = -\rho\, v\, \partial T/\partial x - p/c_v\, (\partial v/\partial x). \tag{4}$$

Using the continuity equation, this can be written as

$$\partial(\rho\, T)/\partial t = -\partial(\rho\, v\, T)/\partial x - p/c_v(\partial v/\partial x). \tag{5}$$

The divergence theorem is applied. The pressure is assumed to be constant in the control volume and can be taken outside the integral. Then

$$\partial/\partial t \int_v (\rho\, T)\, dV = -\int_s (\rho\, v\, T I)\, n\, dS - (p/c_v) \int_s (v I)\, n\, dS \tag{6}$$

The basic variable is the mass times the temperature. This can, as before, be changed by convection (first right-hand term). Hot or cold gas can enter through a boundary. The temperature can also be changed through work (second right-hand term). Note that in the last term, the pressure is not evaluated at the boundary, but is the pressure in the control volume.

The momentum equation in the axial direction is (Bird, Stewart, and Lightfoot 1960)

$$\rho\, \partial v/\partial t = -\rho\, v\, \partial v/\partial x - \partial p/\partial x. \tag{7}$$

The viscosity terms are not included. Viscosity will only be important for shear stress (perpendicular to the direction of flow). For the present 1-D model, this cannot be resolved. Using the continuity equation, this can be rewritten as

$$\partial(\rho v)/\partial t = -\partial(\rho v^2)/\partial x - \partial p/\partial x. \quad (8)$$

Applying the divergence theorem,

$$\partial/\partial t \int_V (\rho v)\, dV = -\int_S (\rho v^2\, I + p I)\, n\, dS. \quad (9)$$

3.2 Grid. Figure 1 shows the grid used in the gun tube. The solid lines represent the vector grid and are labeled from 1 to nt. The grid points are evenly spaced. Midway between the vector grid is the scalar grid, labeled from 1 to nt – 1.

The vector grid splits the chamber up into scalar control volumes. The scalar quantities are assumed to be constant within each scalar volume (between solid lines). There is a discontinuity in the scalar quantities at each solid line. Each scalar volume has a volume V and a gas mass M. The gas in the scalar volume has density $\rho = M/V$, pressure p, and temperature T.

The dotted lines split up the chamber into vector control volumes. The velocities are assumed to be the same through each vector control volume, and there is a jump in velocity at the dotted lines. Each vector control volume is made up of half of two scalar control volumes. The mass in the vector control volume I is half the mass in the scalar control volume $I - 1$ plus half the mass in the scalar control volume I, that is, $M_v(I) = 0.5\,(M(I-1) + M(I))$. The vector control volumes at the boundary require special consideration (see Section 3.4). If the grid spacing exceeds a user-specified value, *dxmax*, an additional grid point is added. A maximum number of grid points, *nmax*, can also be specified.

The grid stretches between the tube entrance and the projectile. The grid velocity $U(nt)$ at the projectile equals the projectile velocity. The grid velocity $U(1)$ at the tube entrance is zero. The other grid velocities are found by linear interpolation. So the grid remains equally spaced as the integration proceeds. At muzzle exit, the grid is attached to the end of the gun tube and all the grid velocities are set equal to zero.

With this formulation, the governing equations can be simplified. Consider the continuity Equation 2 applied over a scalar control volume. The density is constant within the control volume, so it can be taken outside of the left-hand integral. The left-hand side then just becomes density times volume or mass. The right-hand side involves the velocity across the boundaries. Since the boundaries are also moving, this is the difference between the grid and gas velocities. The density must also be known on the boundaries. Upwind differencing is used, which means the density on the boundary is assumed to be the density from the direction of flow. The direction of flow on a boundary is determined by the sign of the gas minus grid velocity, defined as

$$u(l) = v(l) - U(l) . \tag{10}$$

Assuming a positive gas minus grid velocity and using upwind differencing,

$$\partial M(l)/\partial t = \{\rho(l-1)\, u(l) - \rho(l)\, u(l+1)\}\, A \tag{11}$$

where A is the gun tube area (cm^2). If instead the quantity $u(l)$ is negative, the corresponding boundary densities are $\rho(l)$ and $\rho(l+1)$.

Similarly, the energy equation (6) becomes

$$\begin{aligned} \partial[MT](l)/\partial t = {} & \{\rho(l-1)\, T(l-1)\, u(l) - \rho(l)\, T(l)\, u(l+1)\}\, A \\ & + [p(l)/c_v]\, \{v(l) - v(l+1)\}\, A . \end{aligned} \tag{12}$$

The first term on the right-hand side is a convection term, and the appropriate velocity is the velocity across the boundary. The second term is a work term. The change in temperature is due to the compression or expansion of the gas and the appropriate velocity is the gas velocity.

$$\partial[M_v v](i)/\partial t = \{\rho(i-1)\ v(i-1)\ u(i-1) - \rho(i)\ v(i)\ u(i)\}\ A + g_o\ \{p(i-1) - p(i)\}\ A\ , \tag{13}$$

where g_o is a conversion constant (10^7 gm/s-cm-MPa). For this case, the boundaries of a vector control volume are in the middle of the scalar control volumes, so the density and pressure are the same irregardless of the direction of flow. However, the velocity must be found on the velocity control volume boundary, and again upwind differencing is used. The form given in Equation 13 is for flow in the positive direction, which will be the case until late in the blowdown phase.

3.3 Heat Loss. The loss of energy to the gun tube walls has a noticeable effect on the interior ballistics. To compute heat transfer to the wall, a 2-D code is required. Instead, a correlation from the lumped parameter code is implemented.

The gun tube temperature T_w is assumed to remain constant (infinite sink). Then the heat loss can be represented as

$$Q_w = 4h_w(T - T_w)/d \tag{14}$$

where T is the gas temperature in the tube, d is the tube diameter (cm), h_w is the heat transfer coefficient (J/cm^2 – K – s), and Q_w is the heat loss (J/cm^3 – s) (Bird, Stewart, and Lightfoot 1960). The variation of temperature in the gun tube is ignored. The difficulty is in computing the heat loss coefficient. In the code, the correlation of Sieder and Tate for pipe flow is used. This assumes fully developed flow in a smooth pipe with a nearly constant wall temperature. For highly turbulent flow,

$$h_w = (k/d)\ 0.026\ Re^{0.8}\ Pr^{1/3}\ (\nu/\nu_w)^{0.14}\ , \tag{15}$$

where k is the thermal conductivity of the gas (J/cm – K – s), Re is the Reynold's number,

Pr is the Prandtl number, and v is the viscosity (poise = g/cm – s). The correlation is for steady-state flow, while the gun conditions are highly transient. More importantly, the correlation has been found to be accurate for Reynold's numbers up to about 10^5, while Reynold's numbers in the gun tube can be two orders of magnitude higher.

If a HAN-based propellant is completely burned, it will form a mixture of CO_2, H_2O, and N_2. Procedures have been developed to find the viscosity and thermal conductivity of a mixture of gases (Coffee and Heimerl 1981). The procedures were developed for the low-density limit. Fortunately, for high temperatures, the low-density limit is very accurate even for very high pressures (Bird, Stewart, and Lightfoot 1960). Fits were made for the viscosity and thermal conductivity of the gases resulting from HAN1845 between 300 K and 3,000 K. Values for other HAN-based propellants are almost the same. A separate low temperature fit was made to determine the viscosity at the gun tube wall v_w. The fits are

$$\begin{aligned} v &= 2.3275\ 10^{-6}\ T^{0.74694} \\ v_w &= 5.3083\ 10^{-7}\ T^{0.99566} \\ k &= 1.7974\ 10^{-6}\ T^{0.91880}. \end{aligned} \tag{16}$$

The Reynold's number is given by

$$Re = \rho v d/v \tag{17}$$

and the Prandtl number by

$$Pr = c_p v/k\ , \tag{18}$$

where c_p is the specific heat at constant pressure.

In the lumped parameter code, the correlation is applied to the tube as a whole, using space mean values for ρv and T. In the 1-D code, the correlation is applied to each scalar control volume.

Note that in the actual thermal management code, a different correlation is used for heat transfer, and the gun tube can change temperature. The effects of these inconsistencies has not yet been studied.

3.4 Boundary Conditions. As usual, the flow into the gun tube is assumed to be steady-state isentropic flow (Coffee 1988). This gives the mass flow into the tube. A scalar control volume is set up just to the left of the gun tube ($i = 0$). The density and pressure in this control volume is set equal to the density and pressure just inside the tube (at scalar control volume $i = 1$). The temperature is set equal to the chamber gas temperature, so that mass times temperature is conserved by flow across the boundary. Then the gas velocity at the entrance is given by

$$v(1) = mf/[\rho(0)\,A]\ , \tag{19}$$

where mf is the mass flux (g/s).

Before muzzle exit, the velocity at the right-hand side of the tube is just the projectile velocity. For the scalars, a reflection condition is imposed (i.e., the density, temperature, and pressure just outside the region of integration [$i = nt$] is equal to the scalars just at the end of the physical tube [$i = nt - 1$]).

At muzzle exit, the grid is attached to the end of the gun tube. The flow out of the tube is assumed to be steady-state isentropic flow. If the outflow velocity is larger than the local sound speed, it must be lowered to the sonic velocity (choked flow). The flow will be choked for most of the blowdown phase.

For isentropic flow, the relevant equations are the following. The first law of thermodynamics

$$h + v^2/2g_o = constant\ , \tag{20}$$

where h is the gas enthalpy (j/g) and v is the gas velocity (cm/s). The isentropic process equation

$$p\ (1/\rho - b)^{\gamma} = constant\ , \tag{21}$$

where p is the pressure (MPa), ρ is the density (g/cm^3), b is the covolume (cm^3/g), and γ is the ratio of specific heats. The equation of state is

$$\rho\ R_s\ T = p(1 - b\rho)\ , \tag{22}$$

where T is the temperature (K), and R_s is the specific gas constant (j/g – K). Also required is the equation for the speed of sound in a gas,

$$c^2 = g_o\ \gamma\ p/[\rho(1 - b\rho)]\ , \tag{23}$$

and the enthalpy equation,

$$h = c_p\ T + bp, \tag{24}$$

where c_p is the specific heat at constant pressure (j/g – K).

Let p_r, ρ_r, and T_r be the scalar quantities in the scalar control volume at the end of the gun tube, and v_r the gas velocity at the vector grid point just before the muzzle exit. The problem is then finding the quantities p_t, ρ_t, T_t, and v_t at the throat. The velocity v_t is assumed to be the velocity exactly at the end of the tube. The scalar quantities are the values in the control volume just outside the tube.

Suppose the throat pressure is known. The throat density is found by the process equation. The temperature is found from the equation of state. Then from Equations 20 and 24,

$$v_t^2 = v_r^2 + 2g_o\{c_p(T_r - T_t) + b(P_r - P_t)\}. \tag{25}$$

Previously, the interest has been in subsonic flow. In this case, the throat pressure can just be taken as the pressure just outside the throat (in this case, as 1 atm). However, when the flow reaches the local speed of sound (in the throat), the flow becomes choked, and no further increase in the pressure drop will have any effect. The gas cannot move away fast enough, and a higher pressure region will exist just outside the gun tube. The pressure at which the flow becomes choked is called the critical pressure.

For an ideal gas, the critical pressure can be found analytically. Let the mach number M = v/c. Define the stagnation pressure p_o as the pressure obtained when a gas is decelerated isentropically to zero velocity. Then (Fox and McDonald 1985)

$$p_o = p\{1 + (\gamma - 1)\, M^2/2\}^{\gamma/(\gamma-1)}. \tag{26}$$

Then the critical pressure p_c is given by

$$p_c = p_o\{1 + (\gamma - 1)/2\}^{-\gamma/(\gamma-1)}. \tag{27}$$

The procedure is to find the critical pressure based on the conditions at the right end of the tube. If the critical pressure is less than the exit pressure, the flow is subsonic, and the exit pressure is used as the throat pressure. If the critical pressure is greater than the exit pressure, the flow is choked, and the critical pressure is used as the throat pressure.

For the Noble-Abel equation of state, the relevant equation becomes transcendental, and the critical pressure cannot be found analytically. Instead, an iterative procedure is used. The

ideal gas law critical pressure is computed as a starting point. Using this as the throat pressure, p_t, ρ_t, T_t, v_t, and c_t are computed. If the gas velocity v_t is less than the sound speed, p_t is decreased by an amount proportional to the difference in the velocities. If v_t is greater than c_t, p_t is increased. The ideal gas law critical pressure is a good approximation, so convergence is rapid.

There is one last problem. The mass flow out of the gun tube should be $\rho_t v_t A$, where A is the area of the tube. However, the code uses upwind differencing, so the normal procedure would give a mass flow of $\rho_r v_t A$. So special logic is included at the end of the tube to obtain the proper mass flux out.

Late in the blowdown phase, the pressure inside the tube can become lower than atmospheric pressure. In that case, there is flow into the tube. The gas outside the tube is assumed to be stagnant, since there is no simple way to compute its velocity.

On the other hand, flow from the chamber into the tube is assumed to always be positive, since back flow has not previously been important. If the conditions indicate back flow, the mass flux is just set to zero. This has not been considered important enough to update.

3.5 Time Step. To take a time step, the time derivatives of the lumped parameter quantities are first evaluated and stored in a vector YDOT. The time step *dt* is a user-specified parameter. Copies of the lumped parameter values are stored in a vector *Y*. This is updated using the Euler formula,

$$Y = Y + YDOT*dt \quad . \tag{28}$$

However, the actual lumped parameter values are not updated, so the code is fully explicit.

To take a tube time step, the boundary conditions are applied to find the velocity at the tube entrance and at the projectile. Next, the heat loss term is applied to the energy equation, i.e.,

$$M\,T = M\,T - Q_w\,V\,dt/c_v\,. \tag{29}$$

Other than heat loss to the walls, thermal conductivity is neglected.

Then the Lagrange part of the time step is taken. That is, the grid is momentarily assumed to move at the same velocity as the gas. The continuity and energy equations are unchanged, since there is no mass flow through the boundaries. For the momentum equation, the work term is computed

$$[M_v v]\,(i) = g_o\,\{p\,(i-1) - p(i)\}\;\;A\,. \tag{30}$$

The mass M_v in the vector volume remains unchanged. The velocities are updated by

$$v(i) = [M_v v]\,(i)/M_v(i)\,. \tag{31}$$

The boundary conditions are then updated.

The scalar control volumes have a new Lagrange volume,

$$V_1(i) = V(i) + \{v(i+1) - v(i)\}\,A\;\,dt\,. \tag{32}$$

The new density is given by

$$\rho\,(i) = M(i)/V_1\,(i). \tag{33}$$

The temperature equation is updated using the work term

$$[M\,T](i) = [M\,T](i) - [p(i)/c_v]\,[V_1 - V]\ , \tag{34}$$

and the new temperature is now

$$T(i) = [M\,T](i)/M(i)\ . \tag{35}$$

Finally, the grid is moved to its proper position. The values needed on the boundaries can now be found using upstream differencing. Assuming that *u(i)* is positive everywhere, the advection part of the equations are

$$M(i) = M(i) + \{\rho(i-1)\ u(i) - \rho(i)\ \ u(i+1)\}\ A \tag{36}$$

$$[M\,T]\,(i) = [M\,T]\,(i) + \{\rho\,(i-1)\ T(i-1)\ u(i) - \rho(i)\ T(i)\ u(i+1)\}\ A \tag{37}$$

$$[M_v\,v]\,(i) = [M_v\,v]\,(i) + \{\rho\,(i-1)\ v(i-1)\ u(i-1) - \rho(i)\ v(i)\ u(i)\}\ A\,. \tag{38}$$

The boundary conditions are called again and the scalars are updated. The pressure is obtained from the equation of state.

Next, the grid is updated. The new position of the grid points is found by applying the grid velocity over the time step. The size of the new control volumes is computed. The acceleration on the projectile is found from the pressure at the right-hand scalar control volume. From the acceleration, the new projectile velocity is found. This then allows the new grid velocities to be computed. If the control volumes are longer than a user-specified length, *dxmax*, a new grid point is added. The grid points are rearranged so the grid spacing is uniform. The velocities on the new grid are found by interpolation. The new scalar control volumes are each made up of parts of two old scalar control volumes. The appropriate

fraction of material from each of the old control volumes is put into the new control volumes, and the boundary conditions are updated. Finally, the new values of the lumped parameter variables are updated.

There is a minor numerical problem if the projectile initially has zero offset. In the lumped parameter code, if the projectile is only a short distance downtube, the chamber/tube is treated as one region. This is no longer desirable, since the chamber can have liquid and the tube cannot. So instead, a minimum offset of 0.01 cm is assumed. However, suppose a moderate-sized time step is taken. The mass flux into the tube is constant over the time step. Since the tube volume is tiny, the density and pressure will overshoot, leading to numerical problems. So logic was added to allow a smaller time step if the grid spacing is smaller than dxmax.

4. VALIDATION

4.1 Comparison With Lumped Parameter Model. An initial comparison was made with the lumped parameter gun code (Table 1). This can only be done up to muzzle exit.

Table 1. Comparison Between Lumped Parameter and 1-D Models for Round 77

dt (ms)	dxmax (cm)	nmax	v_m (m/s)	Maximum Chamber Pressure (MPa)	Run time (min/s)
Lumped parameter			896	238	12
.01	5	50	917	256	16
.003	5	50	900	238	41
.001	5	50	900	238	1:53
.003	2	200	906	238	1:57
.001	2	200	902	239	5:27
.0003	2	200	901	238	17:32

As a test case, a recent 14-liter (full charge) firing from the General Electric second generation 155-mm gun was used (Round 77) (Coffee and Wren, to be published). This results in a relatively high muzzle velocity (893 m/s), where the differences in the gun tube model are expected to be more important. The projectile travel is just under 7 m.

Several runs were made to check on the convergence properties. The numerical controls are the time step *dt*, the grid spacing *dxmax*, and the maximum number of grid points *nmax*. The calculated muzzle velocities and maximum chamber pressures are given. The calculations were performed on a Silicon Graphics 4D/310 GTX workstation. The results show convergence even with a fairly coarse grid.

Figure 2 compares the chamber pressure from the lumped parameter model and from the two grids used with the 1-D model (smallest time steps from Table 1). The profiles are almost overlays. It is only at late times, when the projectile is far downbore, that the 1-D model shows differences from the lumped parameter model. Figure 3 shows the corresponding curves for the projectile velocities.

Figures 4–7 compare the gun tube profiles near the end of the firing cycle at 18 ms. Overall, the two 1-D models are in very close agreement, indicating that grid independence has been reached. The 1-D code shows higher velocities, but the velocity at the projectile is almost the same as from the lumped parameter model. The pressure curve from the 1-D model shows less curvature than the lumped parameter model. However, both models predict a pressure difference of approximately 5 MPa from the tube entrance to the projectile. The density and temperature profiles in the gun tube are somewhat more complicated. There is a low-density region behind the projectile, since the motion of the projectile expands the gas. The pressure equilibrates faster than the density, so the temperature goes up. On the other hand, in a slower projectile case, there is instead a high-density region just behind the projectile. The flow from the chamber tends to increase the density, and the motion of the projectile decreases the density. The competition between these two effects can lead to somewhat complicated behavior near the projectile.

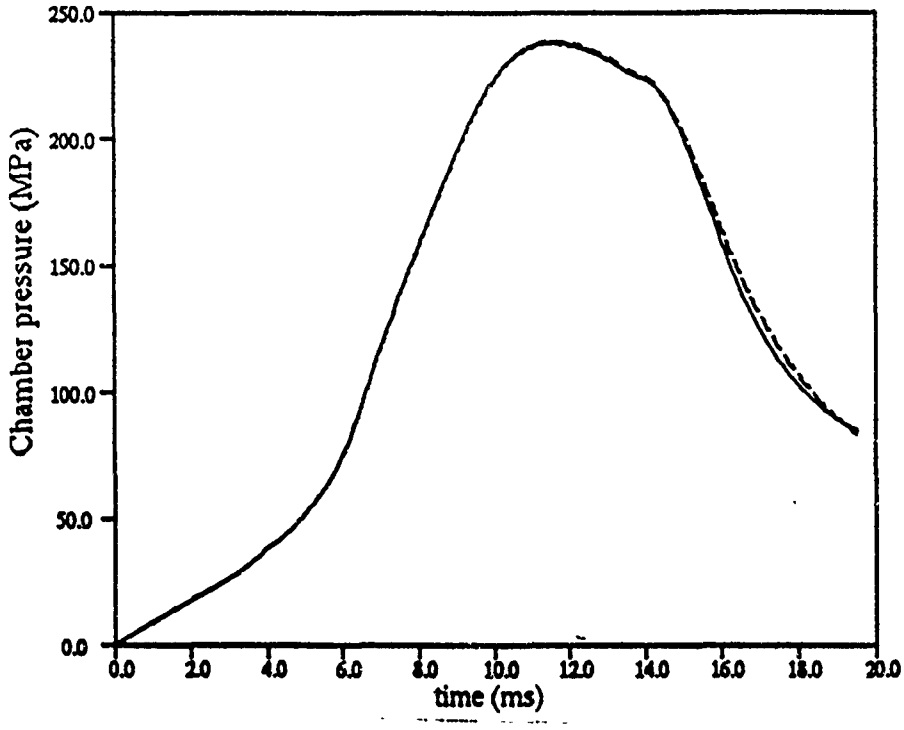

Figure 2. Round 77. Chamber Pressure. Lumped Parameter Model (Line). Coarse Grid (Dot). Finer Grid (Dash).

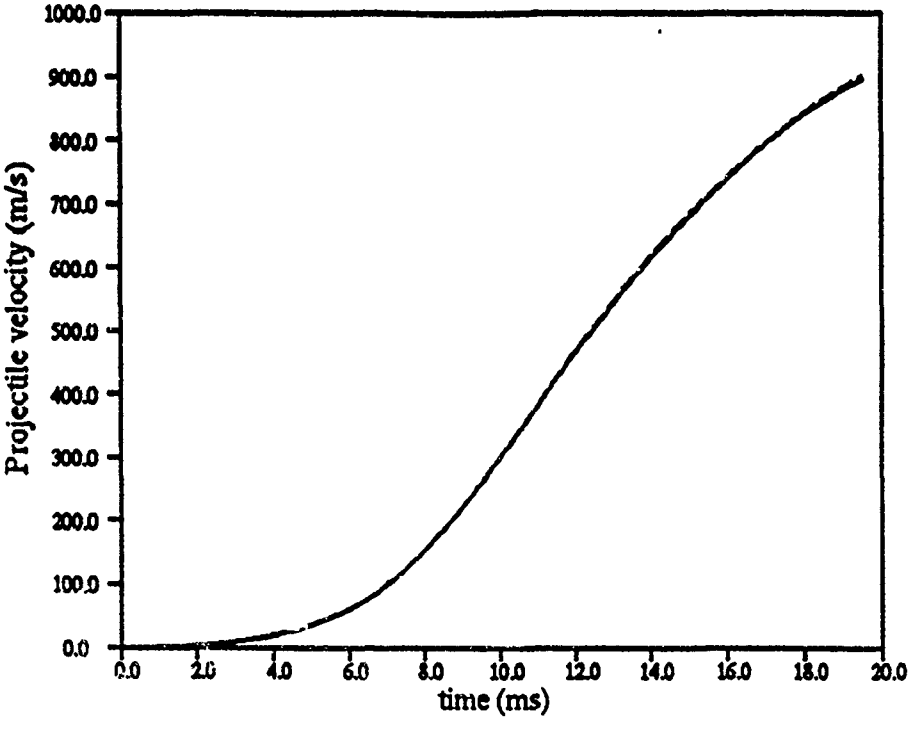

Figure 3. Round 77. Projectile Velocity. Lumped Parameter Model (Line). Coarse Grid (Dot). Finer Grid (Dash).

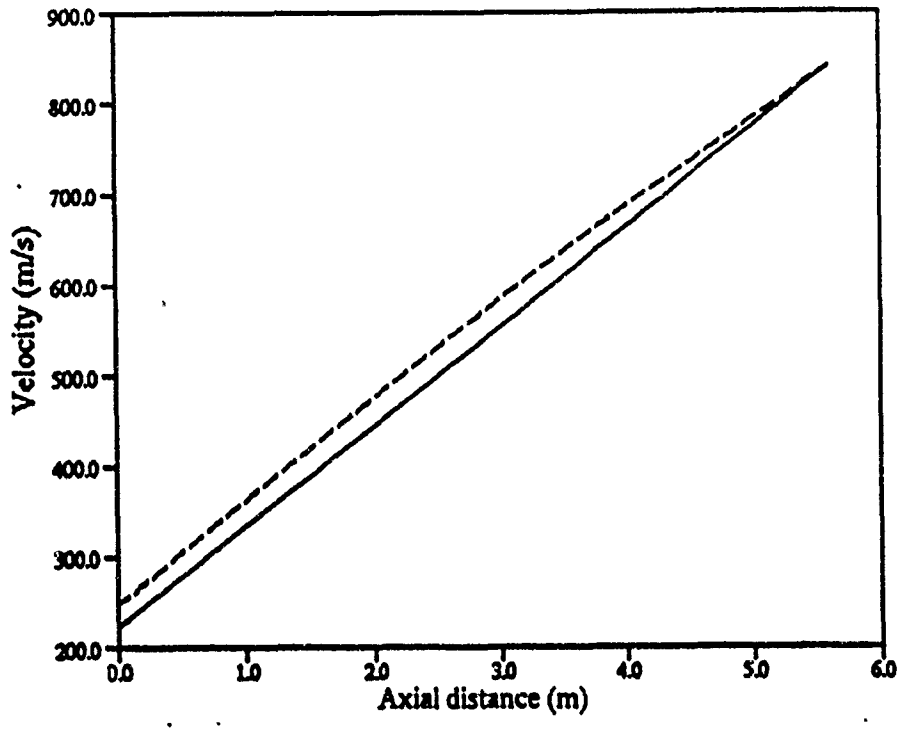

Figure 4. Round 77. Gun Tube Gas Velocity, Time = 18 ms. Lumped Parameter Model (Line). Coarse Grid (Dot). Finer Grid (Dash).

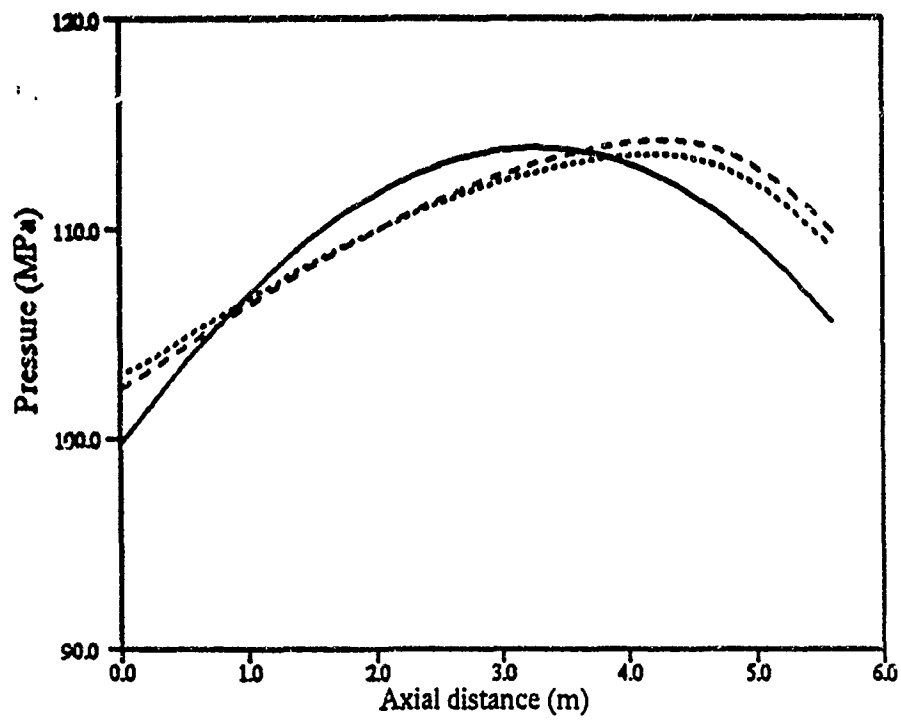

Figure 5. Round 77. Gun Tube Gas Pressure, Time = 18 ms. Lumped Parameter Model (Line). Coarse Grid (Dot). Finer Grid (Dash).

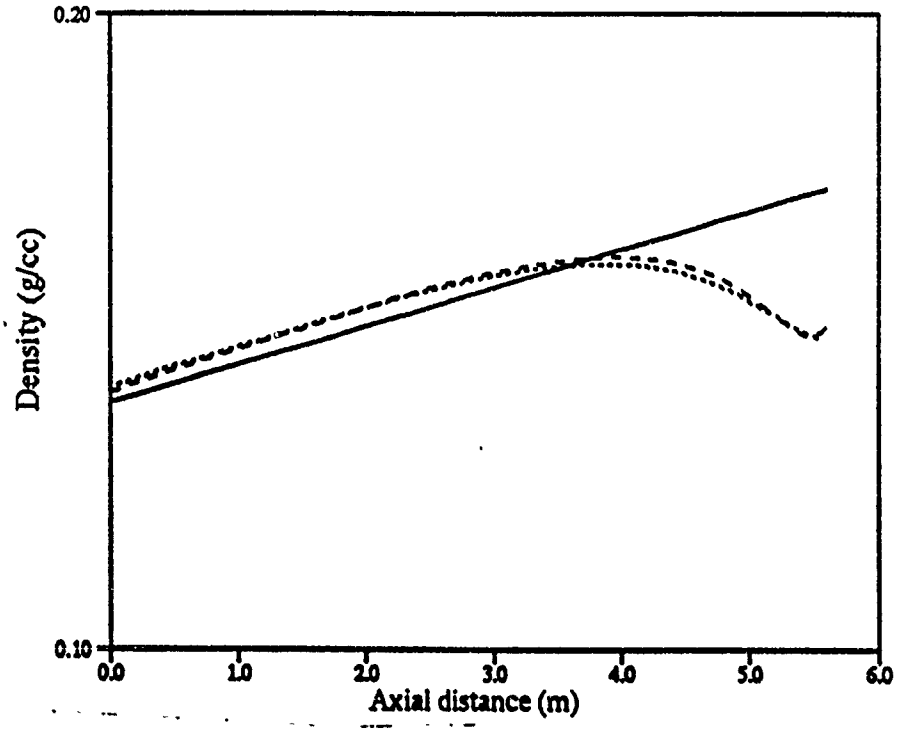

Figure 6. Round 77. Gun Tube Gas Density, Time = 18 ms. Lumped Parameter Model (Line). Coarse Grid (Dot). Finer Grid (Dash).

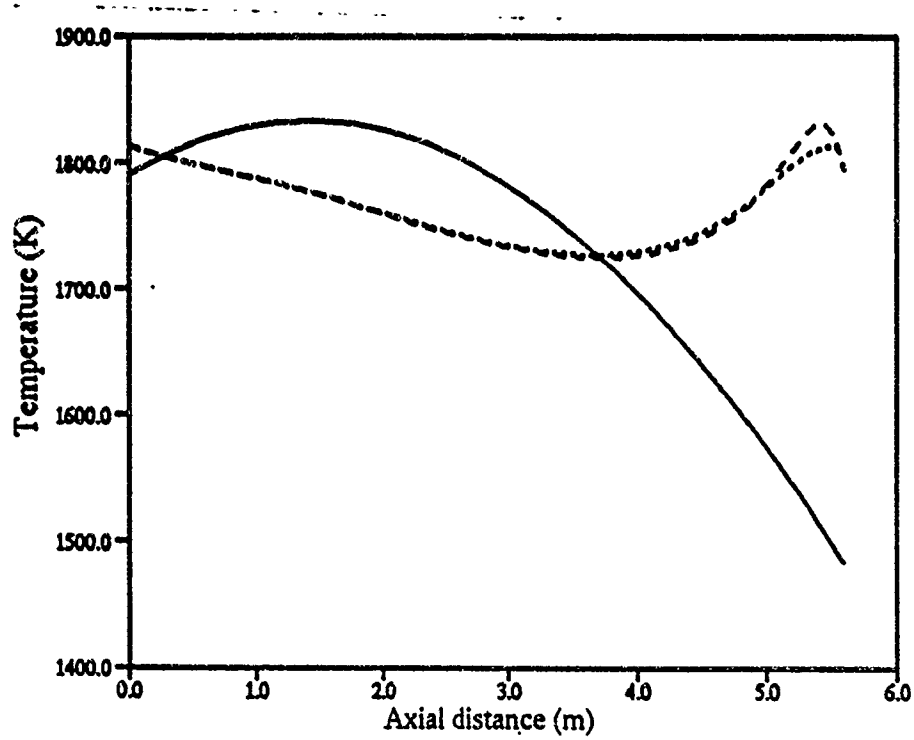

Figure 7. Round 77. Gun Tube Gas Temperature, Time = 18 ms. Lumped Parameter Model (Line). Coarse Grid (Dot). Finer Grid (Dash).

Comparisons were also made for a 30-mm system, a 105-mm system, and smaller charge 155-mm systems. The agreement between the lumped parameter code and the 1-D code was better than that reported above.

4.2 Comparison With Theory. Experimental data for the blowdown phase is not available for liquid propellant guns. So a comparison is made with a theoretical model developed by Corner (1950).

The Corner model assumes that the propellant is totally burned before the projectile starts moving. The gas then expands adiabatically until muzzle exit. It is assumed that the pressure follows a standard Lagrange gradient. A rarefaction wave develops and moves back toward the breech. Corner developed expressions for the profiles from the breech to the rarefaction wave, as well as a formula for the location of the rarefaction wave. There is not a general formula for the profiles from the rarefaction wave to the muzzle. Corner uses expansions in the quantity charge over projectile mass, and ignores second-order terms, so his expressions are only approximate. The model requires as input the projectile muzzle velocity and the average temperature of the gas in the tube at muzzle exit.

In order to mimic the assumptions of the Corner model in the 1-D code, the mass flow from the chamber to the tube is set to zero. The gun tube is chosen as 60 cm long, with a projectile offset of 10 cm. At time = 0, the gun tube is filled with hot gas at a pressure of 500 MPa. The resulting charge is 762.8 g, and the projectile mass was set at 5,000 grams (charge/mass ratio = 0.25).

The 1-D code was run with a maximum grid spacing of 5 cm, 2 cm, and 1 cm. Muzzle exit takes place at 1.06 ms. Figure 8 compares the velocity profiles some time after muzzle exit. The sharp bend in velocity near the tube exit is an artifact of the model. In the model, steady-state choked flow is set up instantaneously. This leads to a jump in velocity from the grid point just inside the tube to the grid point at the muzzle exit. In fact, there should be some delay in reaching steady-state conditions. Otherwise, agreement is good, although not as good as the previous case. Figure 9 compares the pressure curves. By this point in time, the pressures are low. Again, agreement is reasonable.

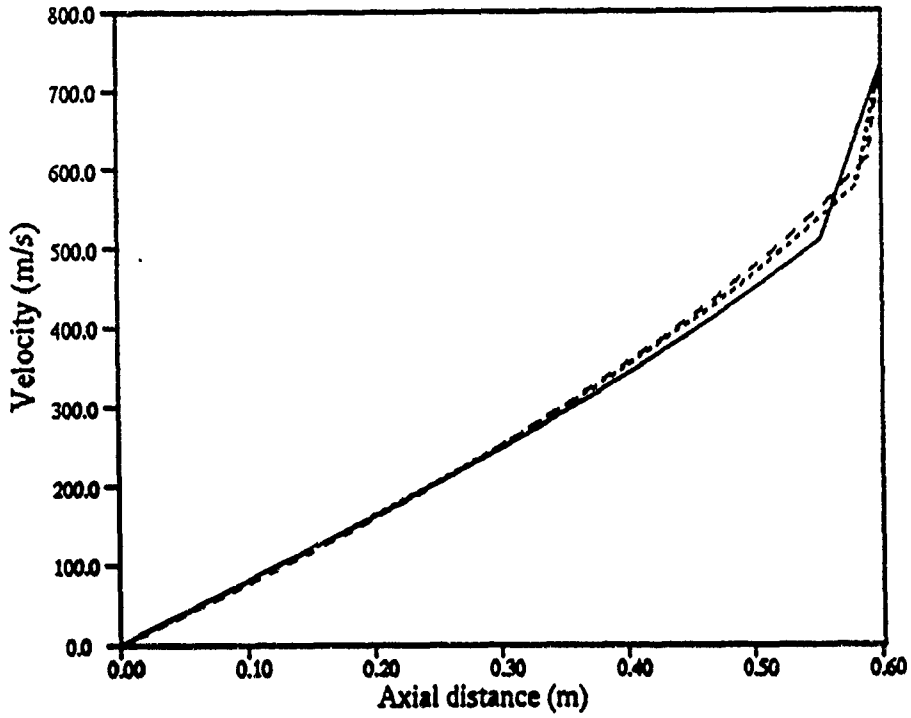

Figure 8. Simple Blowdown. Gun Tube Gas Velocity, Time = 2 ms. Coarse Grid (Line). Medium Grid (Dot). Fine Grid (Dash).

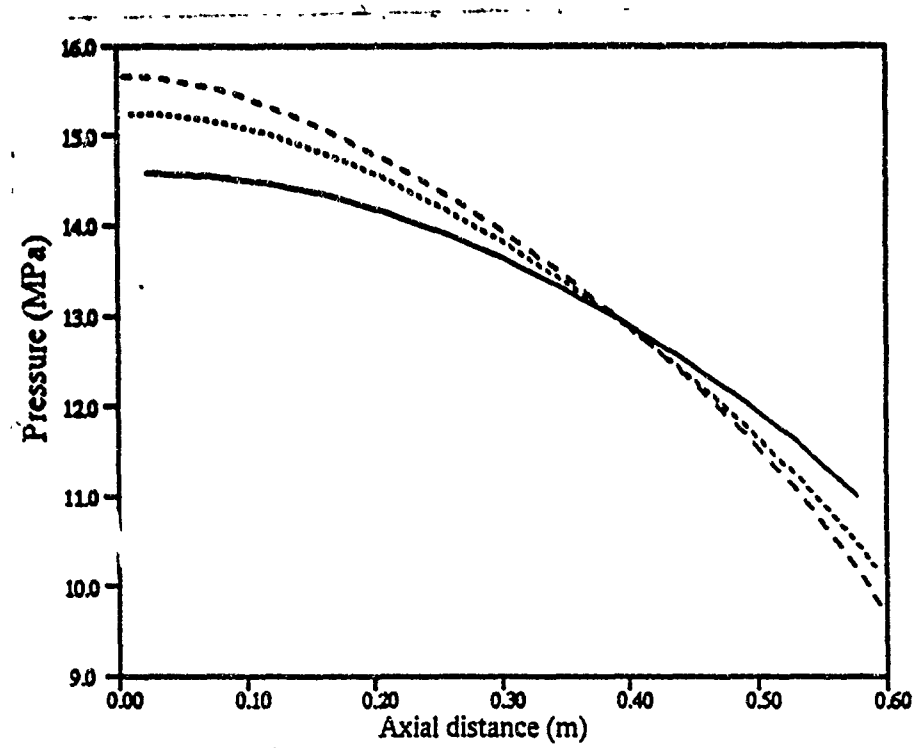

Figure 9. Simple Blowdown. Gun Tube Gas Pressure, Time = 2 ms. Coarse Grid (Line). Medium Grid (Dot). Fine Grid (Dash).

The Corner model is compared to the 1-D simulation with a grid spacing of 1 cm (Figures 10–15). The muzzle velocity and average gun tube temperature at muzzle exit are used as input into the Corner model. At muzzle exit, the 1-D code does show a linear velocity profile. The pressure profiles are fairly flat and agreement is good. Figure 12 compares the velocity profiles some time after muzzle exit. The corner model has a sharp location for the rarefaction wave, while the 1-D code shows a more gradual curvature. The agreement near the tube entrance is still excellent, and the location of the rarefaction wave is about correct. The pressure curve shows similar behavior. At a later time (Figures 14 and 15) the agreement is still good. So the blowdown model is qualitatively showing the proper type of behavior.

5. TEST CASE

The thermal management code was first applied to a simulation of the firing of Unicharge propellant in a 23-liter, 52-caliber cannon, with a projectile travel of 6.9 m. The zone six Unicharge produced a muzzle velocity of about 945 m/s with the 43.54 kg (96 pound) M549 projectile. To make a fair comparison, a liquid propellant simulation was developed that mimicked as closely as possible the Unicharge simulation.

As a starting point, the 14-liter case mentioned in Section 4.1 is used. The projectile offset was reduced to essentially zero (0.01 cm), and the travel extended slightly to 6.9 m. The projectile mass was decreased slightly to the M549 projectile mass. The projectile resistance profiles were changed to that used in the Unicharge simulation. Air shock in front of the projectile was not included. Finally, the damper was adjusted until a muzzle velocity near 945 m/s was obtained.

Again, a series of convergence tests were made (see Table 2). For these tests, the integration was carried out to 50 ms. Muzzle exit occurred at around 17.6 ms.

Figures 16–19 compare the profiles for the three different grid sizes (with the smaller time step) for the profiles at 25 ms. The coarse grid is not completely accurate, but the medium and fine grids show excellent agreement.

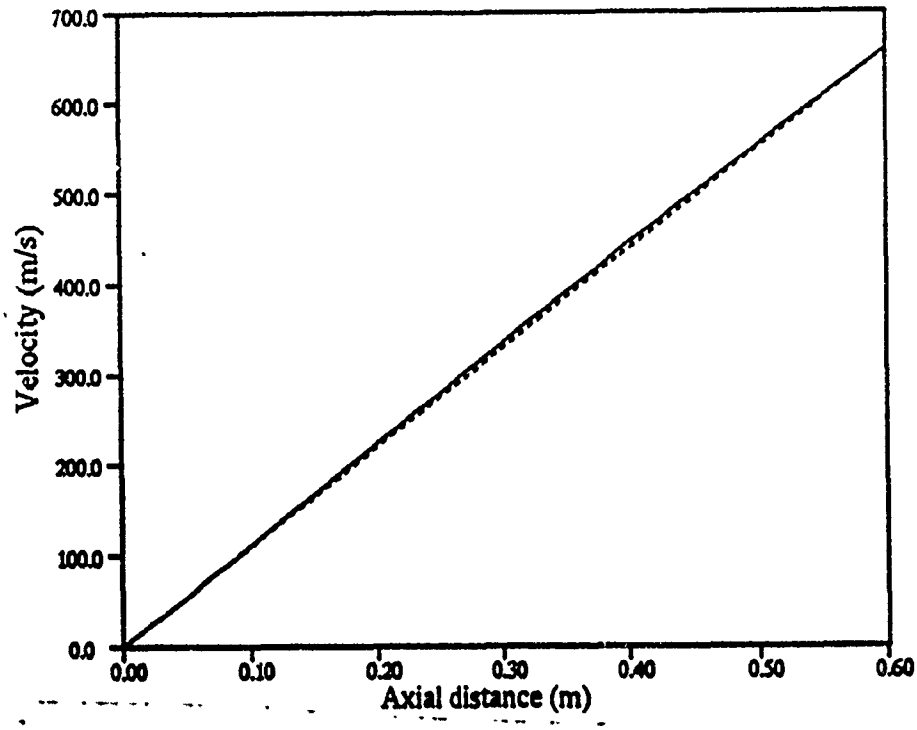

Figure 10. Simple Blowdown. Gun Tube Gas Velocity, Time = 1.06 ms. One-Dimensional Model (Line). Corner Theory (Dot).

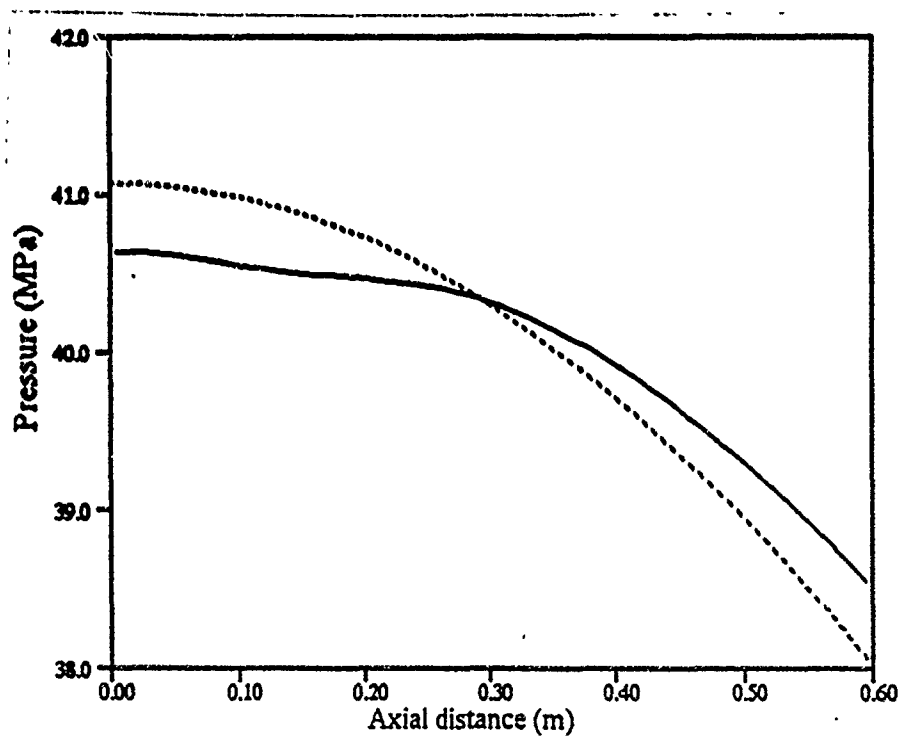

Figure 11. Simple Blowdown. Gun Tube Gas Pressure, Time = 1.06 ms. One-Dimensional Model (Line). Corner Theory (Dot).

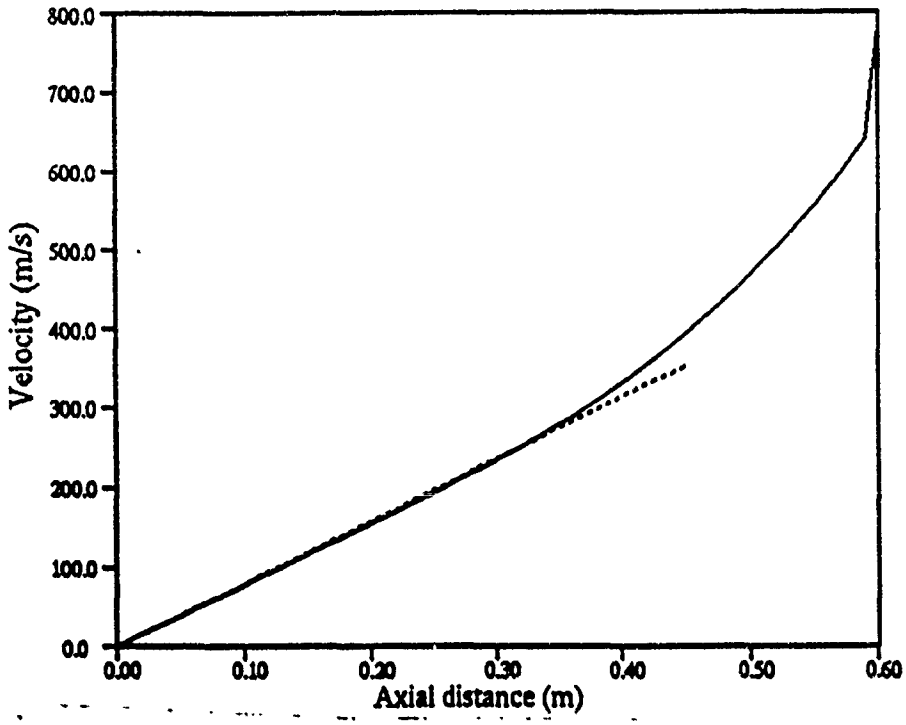

Figure 12. Simple Blowdown. Gun Tube Gas Velocity, Time = 1.5 ms. One-Dimensional Model (Line). Corner Theory (Dot).

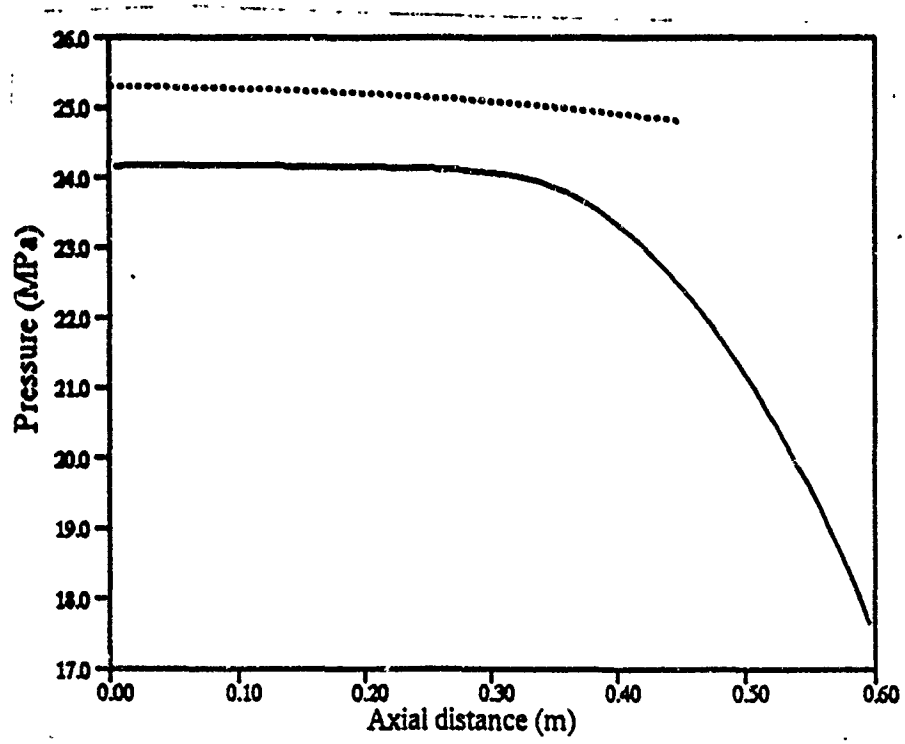

Figure 13. Simple Blowdown. Gun Tube Gas Pressure, Time = 1.5 ms. One-Dimensional Model (Line). Corner Theory (Dot).

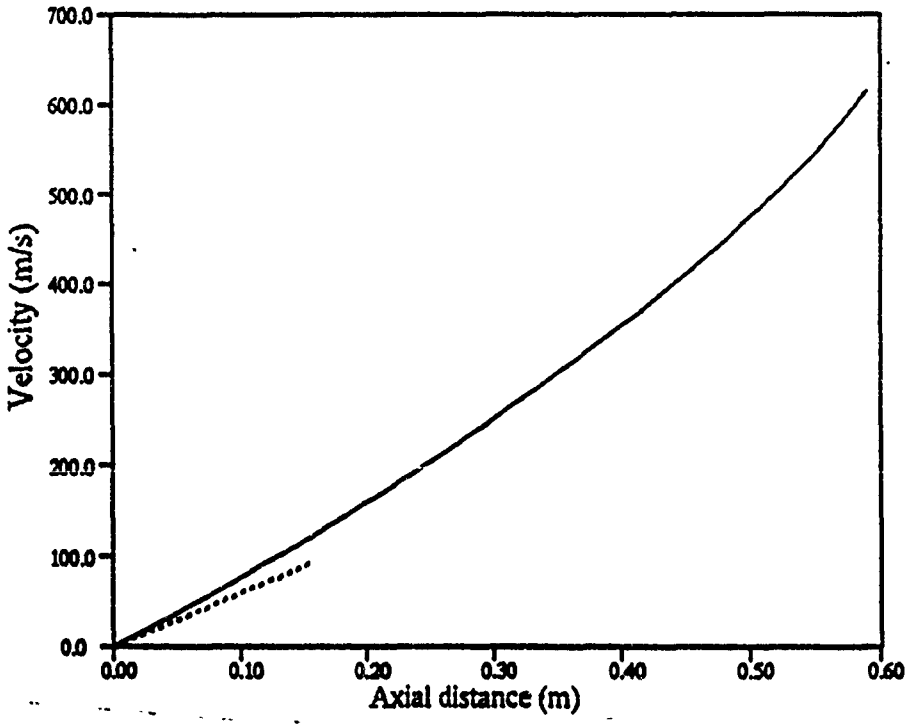

Figure 14. Simple Blowdown. Gun Tube Gas Velocity, Time = 2.0 ms. One-Dimensional Model (Line). Corner Theory (Dot).

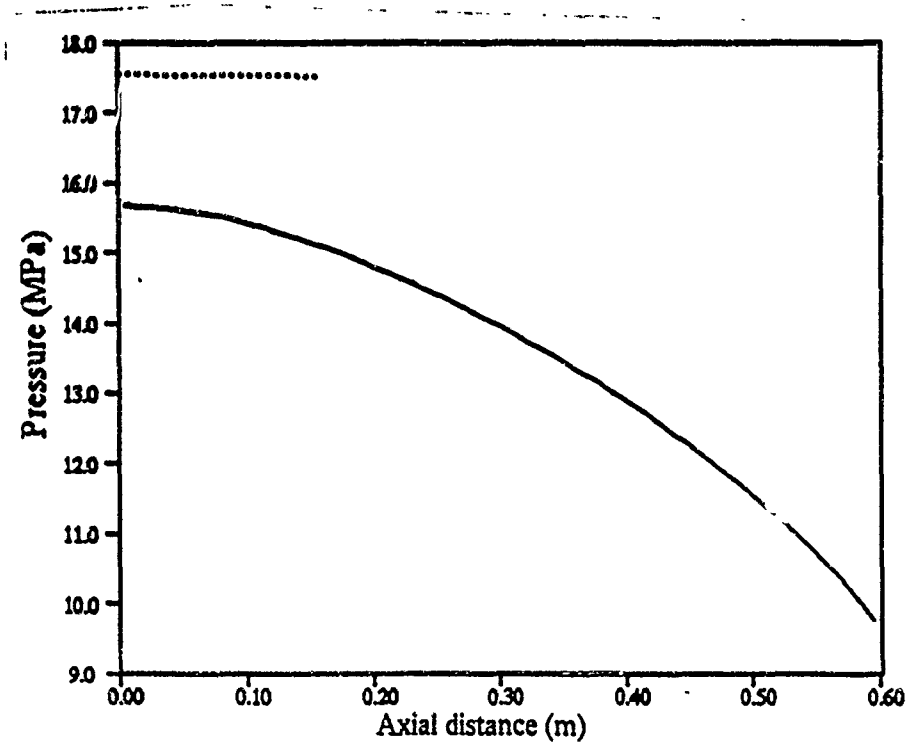

Figure 15. Simple Blowdown. Gun Tube Gas Pressure, Time = 2.0 ms. One-Dimensional Model (Line). Corner Theory (Dot).

Table 2. Comparison Between Lumped Parameter and 1-D Models for Thermal Management Test Case

dt (ms)	dxmax (cm)	nmax	v_m (m/s)	Maximum Chamber Pressure (MPa)	Run time (hr/min/s)
.01	5	50	947	273	1:49
.003	5	50	945	275	3:42
.003	2	200	952	274	10:12
.001	2	200	947	275	27:53
.001	1	500	952	275	1:09:09
.0003	1	500	946	276	3:46:48

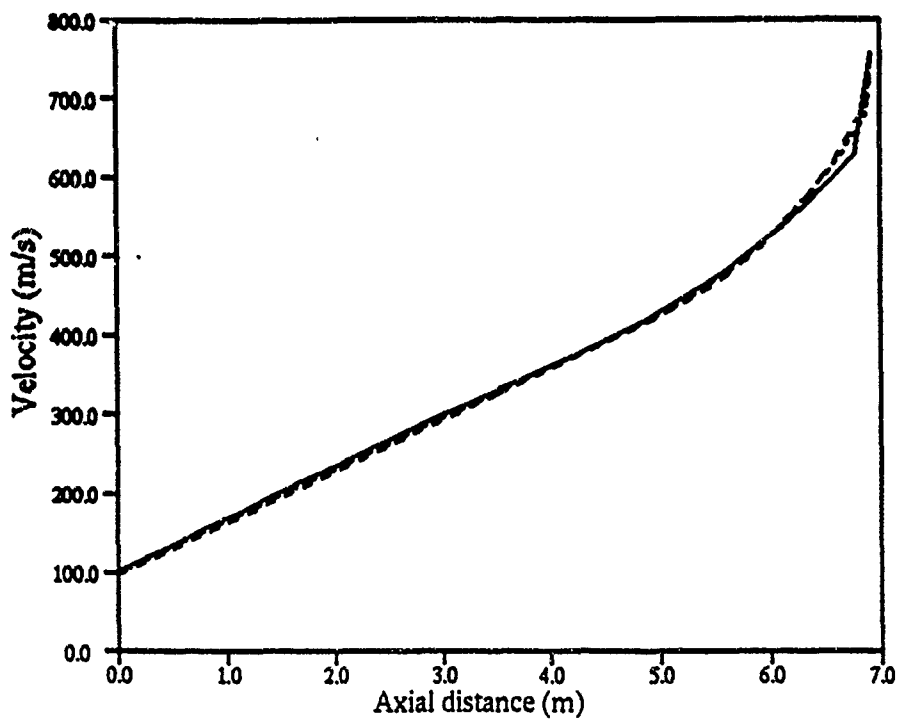

Figure 16. Test Case. Gun Tube Gas Velocity, Time = 25 ms. Coarse Grid (Line). Medium Grid (Dot). Fine Grid (Dash).

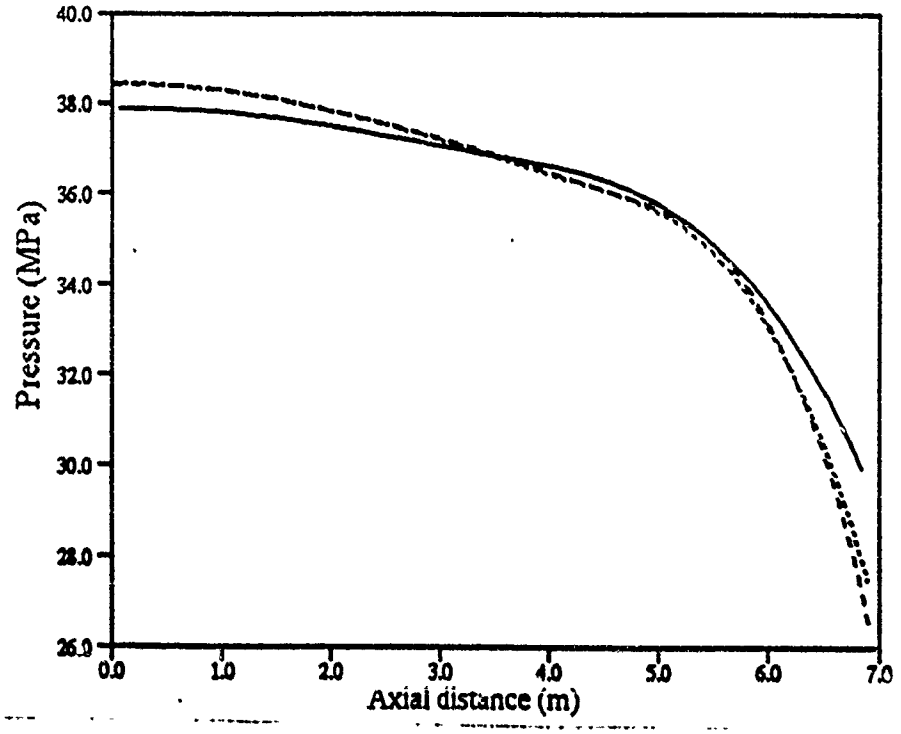

Figure 17. Test Case. Gun Tube Gas Pressure. Time = 25 ms. Coarse Grid (Line). Medium Grid (Dot). Fine Grid (Dash).

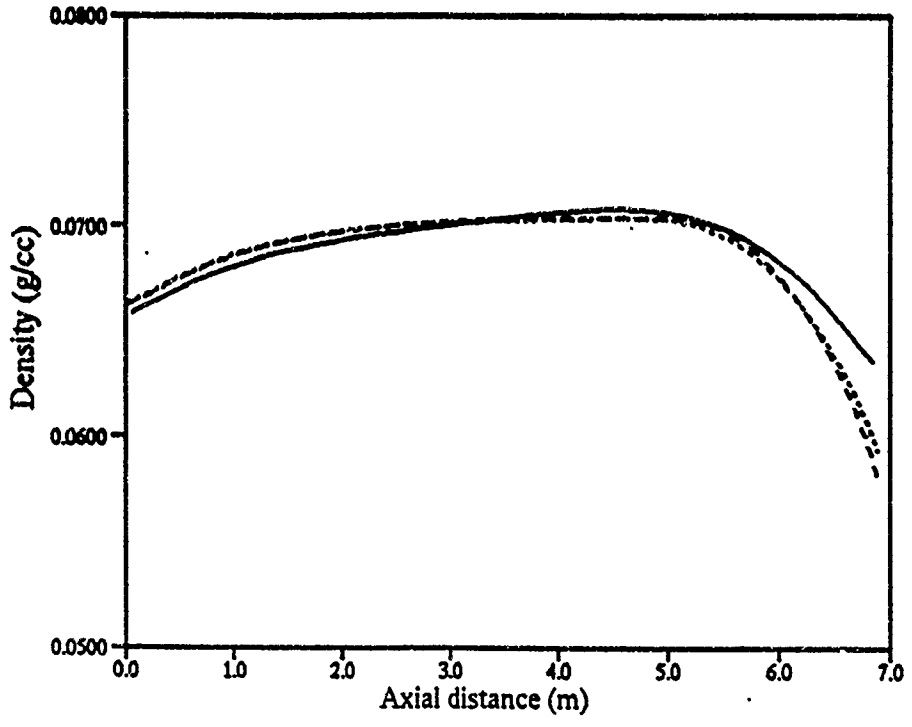

Figure 18. Test Case. Gun Tube Gas Density, Time = 25 ms. Coarse Grid (Line). Medium Grid (Dot). Fine Grid (Dash).

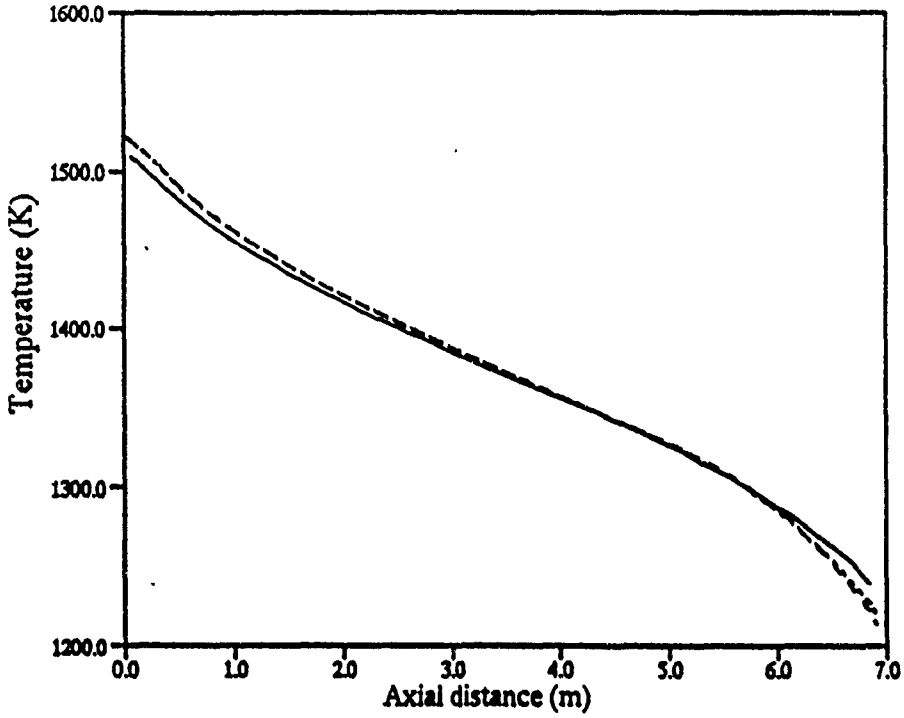

Figure 19. Test Case. Gun Tube Gas Temperature, Time = 25 ms. Coarse Grid (Line). Medium Grid (Dot). Fine Grid (Dash).

For the thermal management simulation (Keller et al. 1991), the integration was carried out to 500 ms. This was to make certain that the gas in the gun tube cooled to near ambient conditions. Significant heat transfer can occur long after muzzle exit as long as the gas in the tube is still hot. For this simulation, the fine grid was used with a time step of .0001 ms. The grid refinement tests reported in Table 2 indicate that this is actually a finer grid and a much smaller time step than required for numerical convergence.

Figure 20 shows the pressures at both ends of the gun tube as a function of time. The pressure essentially reaches atmospheric pressure shortly after 100 ms. Figure 21 shows the corresponding average gas temperature in the gun tube. The temperature increases as the pressure goes up, since the gas is being compressed and hence heated. Once the pressure equilibrates with the outside air, further gas temperature decreases are very gradual. Figure 22 shows the velocity at the right-hand end of the tube simulation. This is the projectile velocity until muzzle exit and the muzzle gas velocity afterwards. For comparison, the space mean sound speed in the tube is also shown. At muzzle exit, by coincidence, the projectile velocity is almost the same as the local speed of sound. So there is no jump in

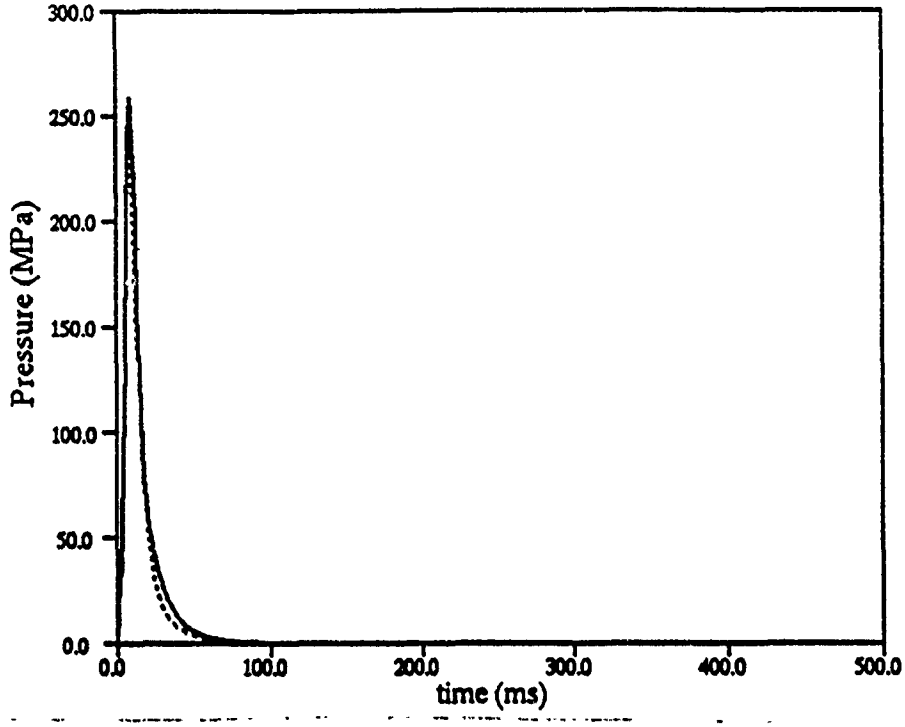

Figure 20. Test Case. Pressure at Left of Tube (Line). Pressure at Right of Tube (Dot).

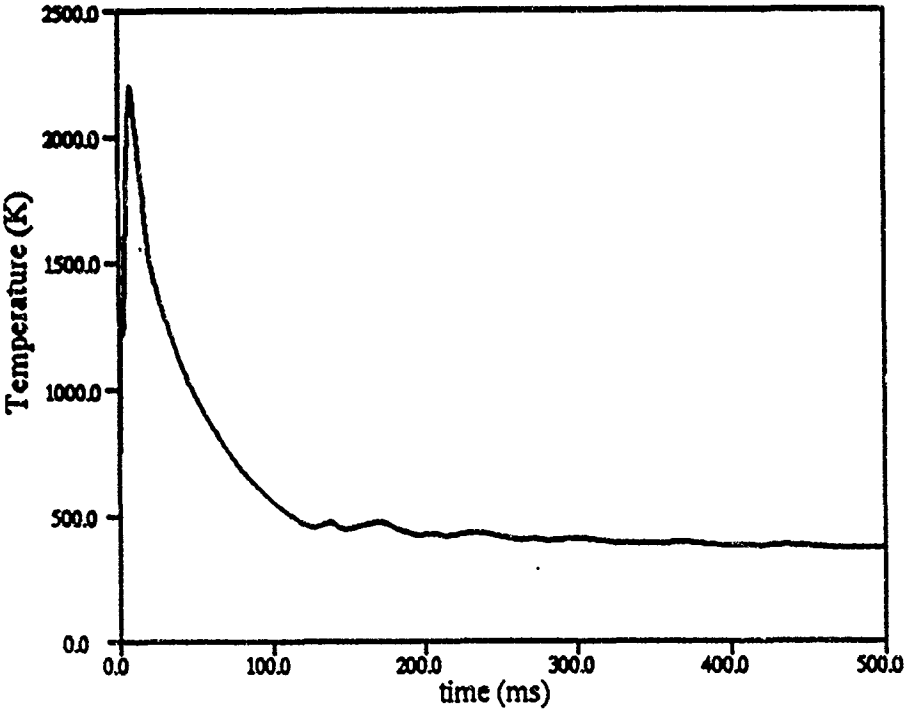

Figure 21. Test Case. Average Gun Tube Gas Temperature.

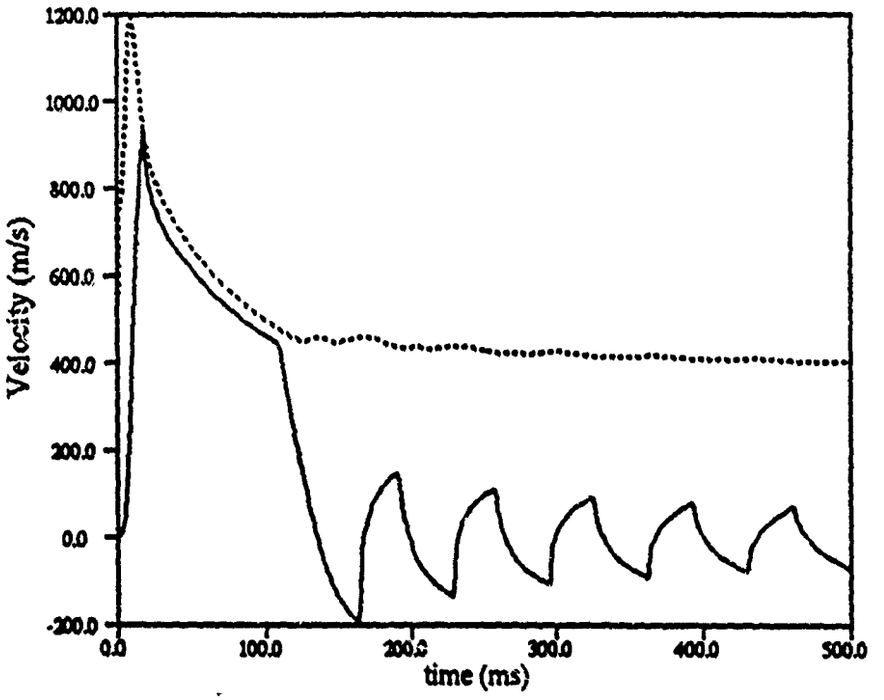

Figure 22. Test Case. Gas Velocity at Right of the Tube (Line). Average Speed of Sound in Tube (Dot).

velocity as steady-state choked flow is established. The flow stays choked until a little after 100 ms. When the flow unchokes, the velocity drops more rapidly. Because of inertia, the pressure in the tube actually becomes less than 1 atm, and the exit velocity becomes negative. Gas then flows in and out of the tube in a gradually damped fashion.

Figure 23 shows the velocity profiles in the tube starting shortly after muzzle exit. The sharp increase in velocity just at the exit is an artifact of the model, since the exit velocity instantaneously reaches the steady-state choked flow velocity. The rarefaction wave propagates very slowly downtube, since the local gas velocity is almost at the speed of sound. Figure 24 shows the velocity profiles at more widely spaced time intervals. The rarefaction wave is damped as it propagates downstream. This is the expected behavior (Corner 1950). Figures 25 and 26 show the corresponding pressure profiles.

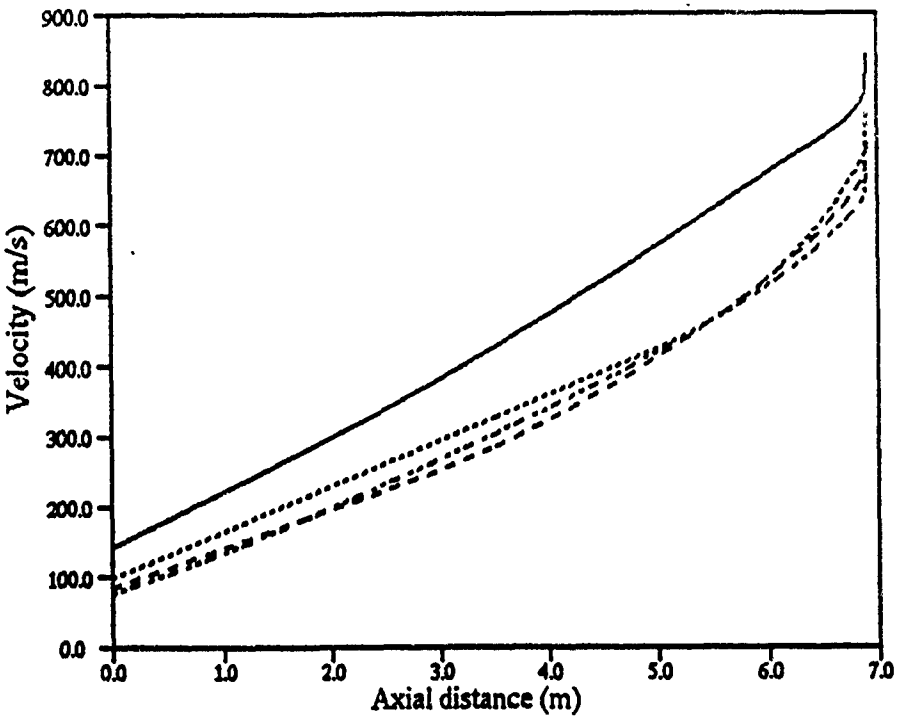

Figure 23. Test Case. Gun Tube Gas Velocity. Time = 20 ms (Line), 25 ms (Dot), 30 ms (Dash), 35 ms (Dot-Dash).

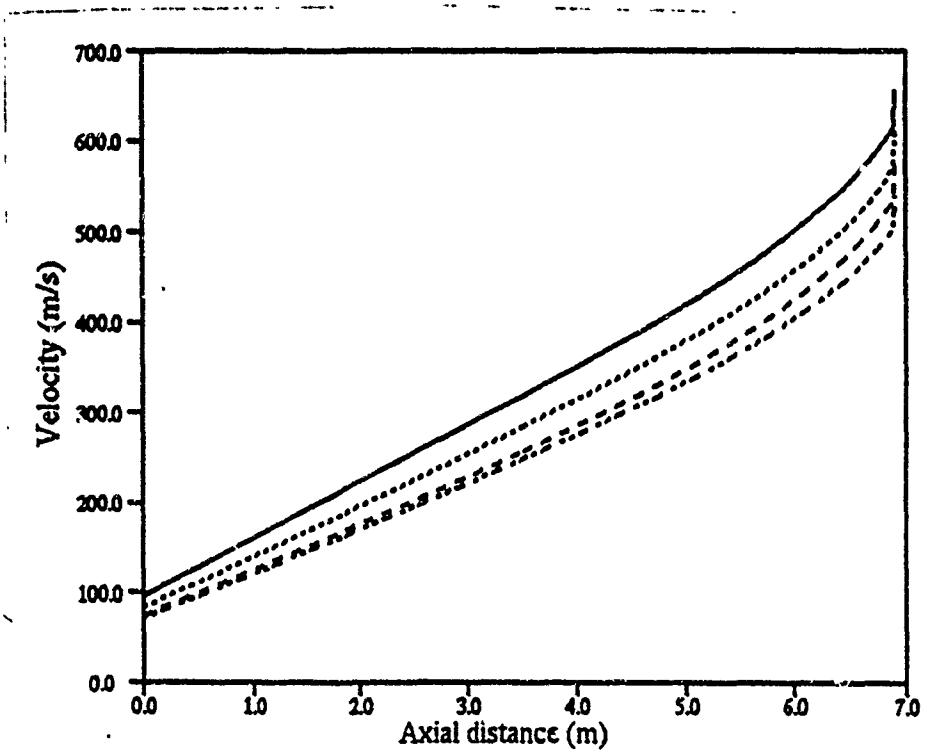

Figure 24. Test Case. Gun Tube Gas Velocity. Time = 40 ms (Line), 50 ms (Dot), 60 ms (Dash), 70 ms (Dot-Dash).

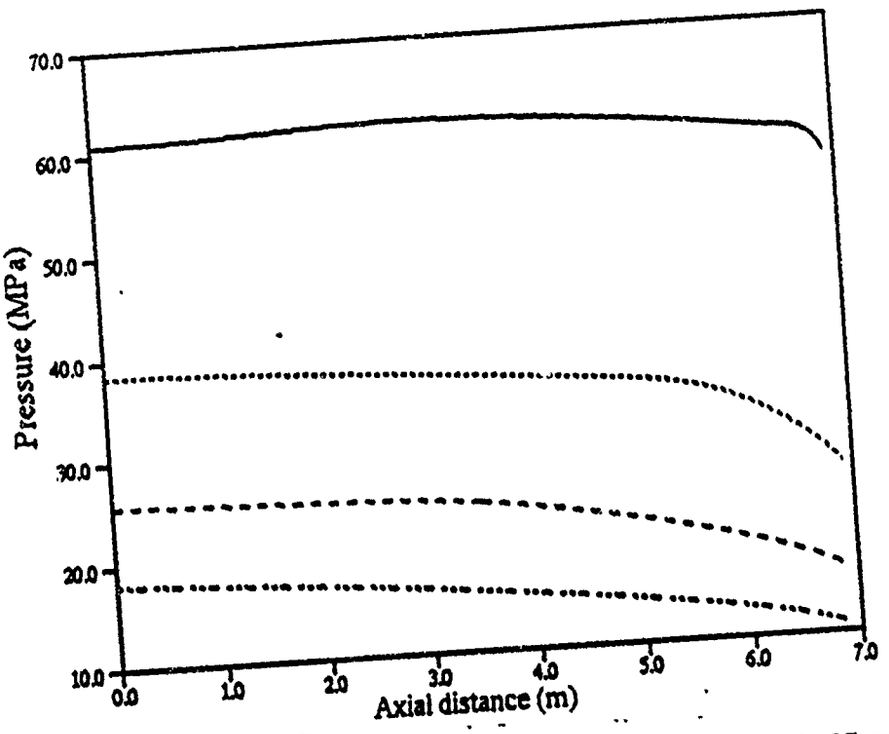

Figure 25. Test Case. Gun Tube Gas Pressure. Time = 20 ms (Line), 25 ms (Dot), 30 ms (Dash), 35 ms (Dot-Dash).

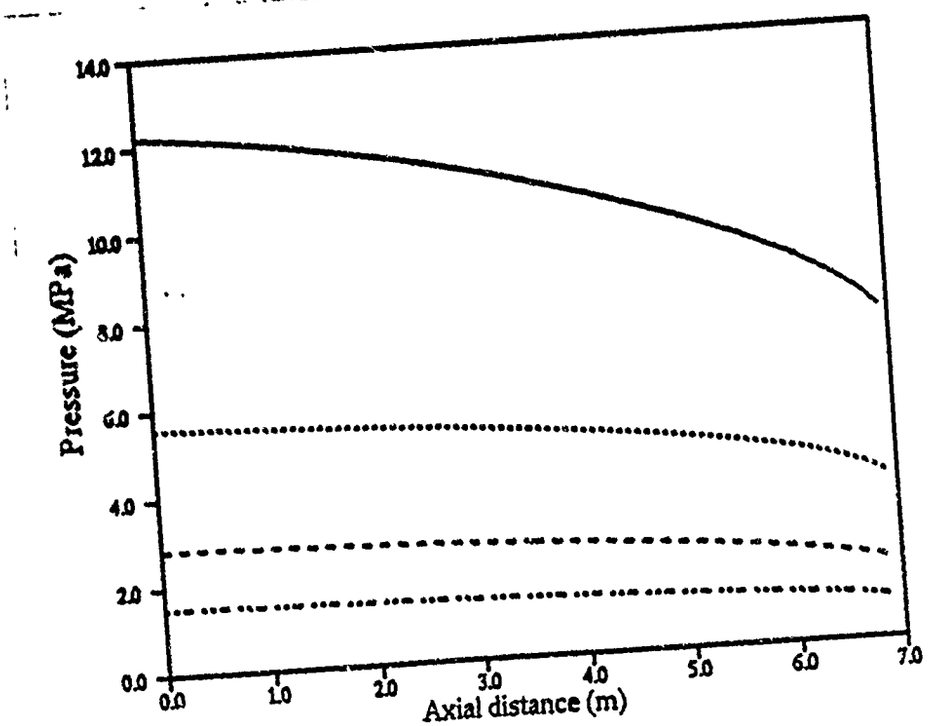

Figure 26. Test Case. Gun Tube Gas Pressure. Time = 40 ms (Line), 50 ms (Dot), 60 ms (Dash), 70 ms (Dot-Dash).

6. CONCLUSIONS

A regenerative liquid propellant gun code which is 1-D in the barrel and lumped parameter elsewhere was developed. Before muzzle exit, the new code agrees very well with the entirely lumped parameter model. After muzzle exit, the results are qualitatively as expected. Combined with a thermal management code to predict wall temperature, the model allows the detailed simulation of barrel heating for liquid propellant guns.

7. REFERENCES

Bird, R. B., W. E. Stewart, and E. N. Lightfoot. Transport Phenomena. John Wiley and Sons, Inc., 1960.

Chandra, S. "Thermal Response Management of Barrels with XBR-2D." Contract No. DAAA15-88-D-0014, Delivery Order 004, U.S. Army Ballistic Research Laboratory, Aberdeen Proving Ground, MD, December 1990.

Chandra S., and E. B. Fisher. "Simulation of Barrel Heat Transfer." Final Report, Contract No. DAAA15-88-D-0014, Delivery Order 002, U.S. Army Ballistic Research Laboratory, Aberdeen Proving Ground, MD, June 1989a.

Chandra S., and E. B. Fisher. "Analysis of 16-inch/50 Gun Chamber Heating." Veritay Report No. C68-1, VSE PO NO. 021664, for Naval Ordnance Station, Indian Head, MD, October 1989b.

Coffee, T. P. "A Lumped Parameter Code for Regenerative Liquid Propellant Guns." BRL-TR-2703, U.S. Army Ballistic Research Laboratory, Aberdeen Proving Ground, MD, December 1985.

Coffee, T. P. "One-Dimensional Modeling of Liquid Injection in a Regenerative Propellant Gun." BRL-TR-2897, U.S. Army Ballistic Research Laboratory, Aberdeen Proving Ground, MD, March 1988.

Coffee, T. P. "An Updated Lumped Parameter Code for Regenerative Liquid Propellant In-Line Guns." BRL-TR-2974, U.S. Army Ballistic Research Laboratory, Aberdeen Proving Ground, MD, December 1988.

Coffee, T. P. "A Two-Dimensional Model for the Combustion Chamber/Gun Tube of a Concept VIC Regenerative Liquid Propellant Gun." U.S. Army Ballistic Research Laboratory, Aberdeen Proving Ground, MD, to be published.

Coffee, T. P., P. G. Baer, W. F. Morrison, and G. P. Wren. "Jet Breakup and Combustion Modeling for the Regenerative Liquid Propellant Gun." BRL-TR-3223, U.S. Army Ballistic Research Laboratory, Aberdeen Proving Ground, MD, April 1991.

Coffee, T. P., and J. M. Heimerl. "Transport Algorithms for Premixed, Laminar Steady State Flames." ARBRL-TR-02302, U.S. Army Ballistic Research Laboratory, Aberdeen Proving Ground, MD, March 1981.

Coffee, T. P., and G. P. Wren. "Prediction of Gun Performance for a Second Generation 155-mm Concept VIC Regenerative Liquid Propellant Gun." U.S. Army Ballistic Research Laboratory, Aberdeen Proving Ground, MD, to be published.

Coffee, T. P., G. P. Wren, and W. F. Morrison. "A Comparison Between Experiment and Simulation for Concept VIC Regenerative Liquid Propellant Guns. I. 30 mm." BRL-TR-3072, U.S. Army Ballistic Research Laboratory, Aberdeen Proving Ground, MD, December 1989.

Coffee, T. P., G. P. Wren, and W. F. Morrison. "A Comparison Between Experiment and Simulation for Concept VIC Regenerative Liquid Propellant Guns. II. 105 mm." BRL-TR-3093, U.S. Army Ballistic Research Laboratory, Aberdeen Proving Ground, MD, April 1990.

Conroy, P. J. "Gun Tube Thermal Management." 27th JANNAF Combustion Meeting, Cheyenne, WY, November 1990.

Corner, J. Theory of the Interior Ballistics of Guns, pp. 364–383, John Wiley and Sons, Inc., 1950.

Fox, R. W., and A. T. McDonald. Introduction to Fluid Mechanics. 3rd Edition, John Wiley and Sons, Inc., 1985.

Gough, P. S. "A Model of the Interior Ballistics of Hybrid Liquid Propellant Guns." BRL-CR-566, U.S. Army Ballistic Research Laboratory, Aberdeen Proving Ground, MD, March 1987.

Gough, P. S. "The NOVA Code: A User's Manual. Description and Use." IHCR 80-8, vol. 1, Naval Ordnance Station, Indian Head, MD, December 1980.

Gough, P. S. "The XNOVKTC Code." BRL-CR-627, U.S. Army Ballistic Research Laboratory, Aberdeen Proving Ground, MD, February 1990.

Keller, G. E., A. W. Horst, P. J. Conroy, G. P. Wren, T. P. Coffee, and S. Chandra. "The Influence of Propulsion Technique and Firing Rate on Thermal Management Problems in Large-Caliber Guns." 28th JANNAF Combustion Meeting, San Antonio, TX, October 1991.

Morrison W. F., and T. P. Coffee. "A Modified Lagrange Pressure Gradient for the Regenerative Liquid Propellant Gun." BRL-TR-3073, U.S. Army Ballistic Research Laboratory, Aberdeen Proving Ground, MD, January 1990.

Wren, G. P., T. P. Coffee, and W. F. Morrison. "A Comparison Between Experiment and Simulation for Concept VIC Regenerative Liquid Propellant Guns. III. 155 mm." BRL-TR-3151, U.S. Army Ballistic Research Laboratory, Aberdeen Proving Ground, MD, September 1990.

Wren G. P., and P. S. Gough. "One-Dimensional Analysis of Base Pressure Oscillations in a Regenerative Liquid Propellant Gun." 28th JANNAF Combustion Meeting, San Antonio, TX, October 1991.

No. of Copies	Organization
2	Administrator Defense Technical Info Center ATTN: DTIC-DDA Cameron Station Alexandria, VA 22304-6145
1	Commander U.S. Army Materiel Command ATTN: AMCAM 5001 Eisenhower Ave. Alexandria, VA 22333-0001
1	Commander U.S. Army Laboratory Command ATTN: AMSLC-DL 2800 Powder Mill Rd. Adelphi, MD 20783-1145
2	Commander U.S. Army Armament Research, Development, and Engineering Center ATTN: SMCAR-IMI-I Picatinny Arsenal, NJ 07806-5000
2	Commander U.S. Army Armament Research, Development, and Engineering Center ATTN: SMCAR-TDC Picatinny Arsenal, NJ 07806-5000
1	Director Benet Weapons Laboratory U.S. Army Armament Research, Development, and Engineering Center ATTN: SMCAR-CCB-TL Watervliet, NY 12189-4050
(Unclass. only)1	Commander U.S. Army Rock Island Arsenal ATTN: SMCRI-TL/Technical Library Rock Island, IL 61299-5000
1	Director U.S. Army Aviation Research and Technology Activity ATTN: SAVRT-R (Library) M/S 219-3 Ames Research Center Moffett Field, CA 94035-1000
1	Commander U.S. Army Missile Command ATTN: AMSMI-RD-CS-R (DOC) Redstone Arsenal, AL 35898-5010

No. of Copies	Organization
1	Commander U.S. Army Tank-Automotive Command ATTN: ASQNC-TAC-DIT (Technical Information Center) Warren, MI 48397-5000
1	Director U.S. Army TRADOC Analysis Command ATTN: ATRC-WSR White Sands Missile Range, NM 88002-5502
1	Commandant U.S. Army Field Artillery School ATTN: ATSF-CSI Ft. Sill, OK 73503-5000
(Class. only)1	Commandant U.S. Army Infantry School ATTN: ATSH-CD (Security Mgr.) Fort Benning, GA 31905-5660
(Unclass. only)1	Commandant U.S. Army Infantry School ATTN: ATSH-CD-CSO-OR Fort Benning, GA 31905-5660
1	WL/MNOI Eglin AFB, FL 32542-5000
	Aberdeen Proving Ground
2	Dir, USAMSAA ATTN: AMXSY-D AMXSY-MP, H. Cohen
1	Cdr, USATECOM ATTN: AMSTE-TC
3	Cdr, CRDEC, AMCCOM ATTN: SMCCR-RSP-A SMCCR-MU SMCCR-MSI
1	Dir, VLAMO ATTN: AMSLC-VL-D
10	Dir, USABRL ATTN: SLCBR-DD-T

No. of Copies Organization

1 Commander
U.S. Army Belvoir R&D Center
ATTN: STRBE-WC,
Technical Library (Vault) B-315
Fort Belvoir, VA 22060-5606

1 Commander
U.S. Army Research Office
ATTN: Technical Library
P.O. Box 12211
Research Triangle Park, NC 27709-2211

1 Director
Benet Weapons Laboratory
U.S. Army Armament Research,
Development and Engineering Center
ATTN: SMCAR-CCB-RA, Julius Frankel
Watervliet, NY 12189-4050

1 Commander
U.S. Army Armament Research,
Development, and Engineering Center
ATTN: SMCAR-CCS-C, T. Hung
Picatinny Arsenal, NJ 07806-5000

2 Commandant
U.S. Army Field Artillery School
ATTN: ATSF-CMW
ATSF-TSM-CN, J. Spicer
Ft. Sill, OK 73503

1 Commandant
U.S. Army Armor Center
ATTN: ATSB-CD-MLD
Ft. Knox, KY 40121

3 Commander
U.S. Army Armament Research,
Development, and Engineering Center
ATTN: SMCAR-FSS-DA, Bldg. 94
J. Feneck
R. Kopmann
J. Irizarry
Picatinny Arsenal, NJ 07806-5000

No. of Copies Organization

11 Commander
U.S. Army Armament Research,
Development, and Engineering Center
ATTN: SMCAR-TSS
SMCAR-AEE-BR, B. Brodman
SMCAR-AEE-B, D. Downs
SMCCAR-AEE-BR,
W. Seals
A. Beardell
SMCAR-AEE-W, N. Slagg
SMCAR-AEE,
A. Bracuti
D. Chieu,
J. Salo
SMCAR-FSS-D, L. Frauen
SMCAR-FSA-S, H. Liberman
Picatinny Arsenal, NJ 07806-5000

1 Commander
Naval Surface Warfare Center
ATTN: D. A. Wilson, Code G31
Dahlgren, VA 22448-5000

1 Commander
Naval Surface Warfare Center
ATTN: J. East, Code G33
Dahlgren, VA 22448-5000

2 Commander
Naval Surface Warfare Center
ATTN: O. Dengel
K. Thorsted
Silver Spring, MD 20902-5000

1 Commander
Naval Weapons Center
China Lake, CA 93555-6001

1 Superintendent
Naval Postgraduate School
Dept. of Mechanical Engineering
ATTN: Library, Code 1424
Monterey, CA 93943

1 OSD/SDIO/IST
ATTN: Dr. Len Caveny
Pentagon
WASH DC 20301-7100

No. of
Copies Organization

1 Commandant
USAFAS
ATTN: ATSF-TSM-CN
Ft. Sill, OK 73503-5600

1 Director
Jet Propulsion Laboratory
ATTN: Technical Library
4800 Oak Grove Dr.
Pasadena, CA 91109

2 Director
National Aeronautics and
Space Administration
ATTN: MS-603,Technical Library
MS-86, Dr. Povinelli
21000 Brookpark Rd.
Lewis Research Center
Cleveland, OH 44135

1 Director
National Aeronautics and
Space Administration
Manned Spacecraft Center
Houston, TX 77058

2 Director
Sandia National Laboratories
ATTN: Dr. Ray Rychnovsky, Div. 8152
Dr. Stuart Griffiths, Div. 8244
P.O. Box 969
Livermore, CA 94551-0969

1 Director
Applied Physics Laboratory
The Johns Hopkins University
Johns Hopkins Rd.
Laurel, MD 20707

1 Univ. of Illinois at Chicago
ATTN: Professor Sohail Murad
Dept. of Chemical Engineering
Box 4348
Chicago, IL 60680

1 University of Maryland at College Park
ATTN: Professor Franz Kasler
Dept. of Chemistry
College Park, MD 20742

No. of
Copies Organization

1 University of Maryland at College Park
ATTN: Professor Franz Kasler
Dept. of Chemistry
College Park, MD 20742

1 University of Missouri at Columbia
ATTN: Professor R. Thompson
Dept. of Chemistry
Columbia, MO 65211

1 University of Michigan
ATTN: Professor Gerard M. Faeth
Dept. of Aerospace Engeering
Ann Arbor, MI 48109-3796

1 University of Missouri at Columbia
Dept. of Physics
ATTN: Professor F. K. Ross
Research Reactor
Columbia, MO 65211

1 University of Missouri at Kansas City
Dept. of Physics
ATTN: Professor R. D. Murphy
1110 East 48th St.
Kansas City, MO 64110-2499

1 Pennsylvania State University
Dept. of Mechanical Engineering
ATTN: Professor K. Kuo
University Park, PA 16802

2 Princeton Combustion Research
Laboratories, Inc.
ATTN: N. A. Messina
M. Summerfield
4275 U.S. Highway One North
Monmouth Junction, NJ 08852

1 University of Arkansas
Dept. of Chemical Engineering
ATTN: J. Havens
227 Engineering Bldg.
Fayetteville, AR 72701

3 University of Delaware
Dept. of Chemistry
ATTN: Mr. James Cronin
Professor Thomas Brill
Newark, DE 19711

No. of Copies Organization

1 University of Texas at Austin
Bureau of Engineering Research
ATTN: BRC EME133, H. Fair
10100 Burnet Rd., Room 1.100
Austin, TX 78758

1 California State University, Sacramento
School of Engineering and Computer Science
ATTN: Dr. Frederick Reardon
6000 J St.
Sacramento, CA 95819-2694

1 University of Colorado at Boulder
Dept. of Mechanical Engineering
ATTN: Dr. John Daily
Engineering Center ME 1-13
Campus Box 427
Boulder, CO 80309-0427

1 Calspan Corporation
ATTN: Tech Library
P.O. Box 400
Buffalo, NY 14225

7 General Electric Ord Sys Div
ATTN: J. Mandzy, OP43-220
R. E. Mayer
W. Pasko
R. Pate
I. Magoon
Lou Ann Walter
J. McCaleb
100 Plastics Ave.
Pittsfield, MA 01201-3698

1 IITRI
ATTN: Library
10 W. 35th St.
Chicago, IL 60616

1 Paul Gough Associates
ATTN: Paul Gough
1048 South St.
Portsmouth, NH 03801-5423

No. of Copies Organization

1 Science Applications International Corporation
ATTN: Norman Banks
4900 Waters Edge Dr.
Suite 255
Raleigh, NC 27606

1 Sundstrand Aviation Operations
ATTN: Mr. Owen Briles
P.O. Box 7202
Rockford, IL 61125

1 Veritay Technology, Inc.
ATTN: E. B. Fisher
4845 Millersport Hwy.
P.O. Box 305
East Amherst, NY 14051-0305

1 Conway Enterprises
ATTN: Professor Alistair MacPnerson
499 Pine Top Trail
Bethlehem, PA 18017-1828

1 CFD Research Gorporation
ATTN: Dr. Andrzej J. Przekwas
3325-D Triand Blvd.
Huntsville, AL 35805

1 Mr. Paul Baer
2514 Strathmore Ave.
Baltimore, Maryland 21214

No. of
Copies Organization

1 RARDE
GS2 Division
Bldg. R31
ATTN: Dr. Clive Woodley
Ft. Halstead
Sevenoaks, Kent TN14 7BT
ENGLAND

1 Imperial College of Science and Medicine
ATTN: Professor J. H. Whitelaw
Exhibition Rd., London SW7 2BX
ENGLAND

INTENTIONALLY LEFT BLANK.

USER EVALUATION SHEET/CHANGE OF ADDRESS

This laboratory undertakes a continuing effort to improve the quality of the reports it publishes. Your comments/answers below will aid us in our efforts.

1. Does this report satisfy a need? (Comment on purpose, related project, or other area of interest for which the report will be used.) _____

2. How, specifically, is the report being used? (Information source, design data, procedure, source of ideas, etc.) _____

3. Has the information in this report led to any quantitative savings as far as man-hours or dollars saved, operating costs avoided, or efficiencies achieved, etc? If so, please elaborate. _____

4. General Comments. What do you think should be changed to improve future reports? (Indicate changes to organization, technical content, format, etc.) _____

BRL Report Number BRL-TR-3364 Division Symbol _____

Check here if desire to be removed from distribution list. ____

Check here for address change. ____

Current address: Organization _____
Address _____

DEPARTMENT OF THE ARMY
Director
U.S. Army Ballistic Research Laboratory
ATTN: SLCBR-DD-T
Aberdeen Proving Ground, MD 21005-5066

OFFICIAL BUSINESS

BUSINESS REPLY MAIL
FIRST CLASS PERMIT No 0001, APG, MD

Postage will be paid by addressee.

NO POSTAGE NECESSARY IF MAILED IN THE UNITED STATES

Director
U.S. Army Ballistic Research Laboratory
ATTN: SLCBR-DD-T
Aberdeen Proving Ground, MD 21005-5066